Final Report

Project title: Crystallization, Growth, and Morphology Control under High Humidity Condition of 2-Dimensional Perovskite towards Next Generation Optoelectronic Devices

By Dr. Pongsakorn Kanjanaboos

School of Materials Science and Innovation,
Faculty of Science, Mahidol University, Bangkok, Thailand 10400

May 1, 2018

Final Report

Project title: Crystallization, Growth, and Morphology Control under High Humidity Condition of 2-Dimensional Perovskite towards Next Generation Optoelectronic Devices

By Dr. Pongsakorn Kanjanaboos

School of Materials Science and Innovation,
Faculty of Science, Mahidol University, Bangkok, Thailand 10400

Project Granted by the Thailand Research Fund

Abstract

Project Code : MRG59_Pongsakorn Kanjanaboos

Project Title : Crystallization, Growth, and Morphology Control under High Humidity Condition of 2-Dimensional Perovskite towards Next Generation Optoelectronic Devices

Investigator :
Dr. Pongsakorn Kanjanaboos

E-mail Address :
pkanjano@gmail.com

Project Period :
2 May 2016 – 1 May 2018

Abstract:

Over the last few years, the organic-inorganic perovskites ($MAPbI_3$) have attracted considerable attention for application as high-efficiency photovoltaic devices due to their low-cost and low-temperature fabrication compared to conventional solar cells. Good surface morphology and high crystallinity are necessary for high-performance devices. Here, we examine the negative effects of chemical ambiences on perovskite crystal formation and morphology (i.e. pinholes and grain features). The repeated cation doping (RCD) technique was developed to remedy the issues by gradually dropping methyammonium ions, MA^+ on top of about-to-formed perovskite surfaces to cause recrystallization. RCD promotes pinhole-free, compact, and polygonal-like surfaces under various chemical vapor conditions. Furthermore, electronic properties and crystallization are enhanced by RCD. RCD extends its benefits beyond perovskites under vapor ambiences, improving regular perovskites and wasted perovskites.

ในช่วงไม่กี่ปีที่ผ่านมา เพอรอฟสไกท์ชนิดอินทรีย์/อนินทรีย์ดึงดูดความสนใจอย่างมากเนื่องจากมีประสิทธิภาพสูงในการเปลี่ยนพลังงานแสงอาทิตย์เป็นพลังงานไฟฟ้าและยังมีกระบวนการผลิตที่ราคาถูกและใช้อุณหภูมิไม่สูงเทียบกับเซลล์แสงอาทิตย์ชนิดซิลิคอน พื้นผิวที่ดีและความเป็นผลึกที่สูงสำคัญต่อประสิทธิภาพของวัสดุพลังงาน ในงานนี้เราวิจัยผลเสียจากสภาวะไอสารเคมีที่อาจเกิดขึ้นในกระบวนการผลิตและได้พัฒนาวิธีใหม่ที่เรียกว่า repeated cation doping (RCD) โดยวิธีใหม่นี้ทำให้เกิดความเป็นผลึกอย่างช้าๆซ้ำๆ ทำให้ได้พื้นผิวที่แน่นและมีคุณภาพสูง มีความเป็นผลึกและคุณสมบัติทางไฟฟ้าที่ดี กระบวนการRCDช่วยปรับปรุงเพอรอฟสไกท์ในหลายสภาวะทั้งภายใต้ไอสารเคมี ทั้งสภาวะทั่วไป และยังใช้ได้กับเพอรอฟสไกท์ที่ผ่านการใช้มาแล้ว

Keywords : 3-5 words

Perovskite; Perovskite Formation; Crystallization; Ambient Effects; Repeated Cation Doping (RCD); Fabrication Process

Reconditioning Perovskite films under Vapor Environments through Repeated Cation Doping

Chirapa Boonthum[a], Kusuma Pinsuwan[a], Jitprabhat Ponchai[a]

Toemsak Srikhirin[ab], Pongsakorn Kanjanaboos[a]*

[a] School of Materials Science and Innovation, Faculty of Science, Mahidol University, Bangkok, Thailand 10400

[b] Department of Physics, Faculty of Science, Mahidol University, Bangkok, Thailand 10400

Chirapa Boonthum (first author): chirapa.boon@gmail.com

Kusuma Pinsuwan: kusuma.pins@gmail.com

Jitprabhat Ponchai: jitprabhat.pon@gmail.com

Toemsak Srikhirina: toemsak.sri@mahidol.ac.th

Pongsakorn Kanjanaboos (*corresponding author): pongsakorn.kan@mahidol.ac.th

Abstract

Over the last few years, the organic-inorganic perovskites ($MAPbI_3$) have attracted considerable attention for application as high-efficiency photovoltaic devices due to their low-cost and low-temperature fabrication compared to conventional solar cells. Good surface morphology and high crystallinity are necessary for high-performance devices. Here, we examine the negative effects of chemical ambiences on perovskite crystal formation and morphology (i.e. pinholes and grain features). The repeated cation doping (RCD) technique was developed to remedy the issues by gradually dropping methyammonium ions, MA^+ on top of about-to-formed perovskite surfaces to cause recrystallization. RCD promotes pinhole-free, compact, and polygonal-like surfaces under various chemical vapor conditions. Furthermore, electronic properties and crystallization are enhanced by RCD. RCD extends its benefits beyond perovskites under vapor ambiences, improving regular perovskites and wasted perovskites.

Keywords: Perovskite; Perovskite Formation; Crystallization; Ambient Effects; Repeated Cation Doping (RCD); Fabrication Process

1. Introduction

The organic-inorganic perovskite materials have been popular these days because of their excellent semiconductor behaviors coupled with low cost fabrication processes[1]. These hybrid materials have great potentials for modern electronic devices such as Light-Emitting Electrochemical Cells (LECs)[2], Light-Emitting diodes (LEDs)[3] and solar cells[4, 5], having outstanding characteristics i.e. direct bandgap, high charge-carrier mobility, low trap density of electron, and high absorption coefficient[6]. Unlike silicon-based solar cells, these materials can be fabricated through solution processing e.g. spin-coating[7], spray coating[8] and dip-coating[9]. Moreover, perovskite can be expediently prepared from abundant chemical substances and fabricated in low-temperature production[10, 11].

As high power conversion efficiency (PCE) necessitates good morphology and electronic properties, a lot of previous studies have focused on improving perovskite layer through various methods e.g., NaCl-incorporated precursor solution[12], MABr-selective Ostwald ripening process[13], anti-solvent engineering[14, 15], and solvent annealing process[16]. During and after perovskite film formation, perovskite properties are highly sensitive toward surrounding ambient conditions and fabrication protocols[17, 18]. To ensure the success of future large-scale perovskite production, effects of different precursor vapors (i.e. possible leftovers or contaminations) on perovskite morphology and formation are studied in this work. Here, we introduced various potential vapors including gamma-butyrolactone (GBL), dimethyl sulfoxide (DMSO), *N*,*N*-dimethylformamide (DMF) and mixed perovskite precursor vapors (PE) (in 7:3 GBL:DMSO) inside a sealed spinner system during perovskite formation. Film morphology was significantly altered for different vapor ambiences; however, consistent features were observed under repeated trials for the same vapors. Many undesirable features such as pinholes, nonhomogeneousness, and roughness were seen. To overcome this issue, we developed repeated cation doping (RCD) method which slowly drops extra salt mixture such as Methyl ammonium Iodide (MAI) over a fixed period of time on top of about-to-formed perovskite layers to cause gradual recrystallization to improve the perovskite layer. This new technique is a prolonged 1-step deposition unlike the traditional 1-step technique[7, 14, 19, 20], the 2-step technique[21–23], or the combination of 1-step and 2-step techniques[24].

2. Experimental details

2.1 Materials

Lead iodide (PbI_2, 99.95% purity), dimethyl sulfoxide (DMSO, anhydrous grade), g-butyrolactone (GBL, anhydrous grade), *N*,*N*-dimethylformamide (DMF, anhydrous grade), Isopropanol (IPA, anhydrous grade) were all purchased from Sigma-Aldrich. Ethanol (anhydrous grade), toluene (anhydrous grade), and methyl ammonium iodide (MAI) were purchased from Fisher Scientific, Kanto chemical, and Dyesol, respectively.

2.2 Fabrication of perovskite layer

Fluorine-doped tin oxide was cleaned by sonicating in detergent agent, deionized water, and isopropanol, respectively, then soaked in isopropanol overnight. A compact titanium oxide (TiO_2) layer was deposited by a one-step spin deposition at 2000 r.p.m. of 0.3 M titanium (IV) isopropoxide in ethanol solution for 30 seconds, followed by annealing at 450 °C for 1 hour.

Perovskite ($MAPbI_3$) film was fabricated on top of compact TiO_2/ fluorine doped tin oxide. 1.5 M precursor solution was prepared by mixing equimolar ratio of lead iodide (PbI_2) and

methyl ammonium iodide (MAI) in g-butyrolactone (GBL, Sigma-Aldrich)/dimethyl sulfoxide (DMSO, Sigma-Aldrich); 7/3 v/v and stirred at 70 °C for 30 minutes. The perovskite solution was then filtered with a PTFE syringe filter (Whatman, 0.22 um) and spin-coated on a compact TiO_2/ fluorine doped tin oxide substrate. The substrate was spun in a two-speed protocol at 500 r.p.m. for 10 seconds and then 5000 r.p.m. for 60 seconds, followed by toluene dripping[14] at 30th second. The perovskite film was fully crystallized by annealing at 100 °C for 15 minutes.

For the chemical vapor ambient study, the compact TiO_2/ fluorine doped tin oxide substrate was first left in a closed spinner chamber that maintains saturated solvent vapors for 8 minutes. Then, $MAPbI_3$ film was prepared using the same method above.

For the repeated cation doping technique, 3 mL of 0.05 M MAI in ethanol/isopropanol (1/1 v/v) was gradually dropped on top of the about-to-formed perovskite layer (prepared by spinning perovskite solution at 500 r.p.m. for 10 seconds) every 3 seconds for 30 seconds (10 times of dropping) during the second speed protocol (5000 r.p.m. for 60 seconds) through a syringe, followed by toluene dripping at the 33th second. The perovskite film was then annealed at 100 °C for 15 minutes. For RCD with 10 second and 5 second intervals, the same procedure was applied; however, the time intervals between consecutive MAI droppings were 10 seconds (total 3 times) and 5 seconds (6 times), respectively.

A wasted film was prepared by heating perovskite film at 300 °C for 5 minutes; the film was fully changed to the yellowish state. For full doping, 7.8 ml of 0.05 M MAI in ethanol/isopropanol (1/1 v/v) was gradually dropped on top of the wasted film every 3 seconds for 78 seconds (total 26 times of dropping) under the spinning protocol of 5000 r.p.m. for 106 seconds, followed by toluene dripping at 81th second. For the half doping protocol, the MAI solution was reduced to 3.9 ml.

2.3 Characterizations of perovskite materials

The perovskite film morphologies were observed using an scanning electron microscope (Quanta 450 FEI, Tungsten filament electron source, 20 kV, secondary electron (SE) mode). UV-visible absorption spectra were achieved using a uv-vis spectrophotometer (Shimadzu UV-2600, Deuterium lamp light source, double–beam, 1 nm slit width, absorbance mode). X-ray diffraction was performed using a X-ray diffractometer (Advance Bruker, Cu Kα radiation, LYNXEYE high-resolution energy-dispersive 1-D detector, detector scan mode with step size of 0.020449 degree, 0.8 s per step, and theta start of 5.00 degree). The surface photovoltage signals were obtained through a modulated surface photovoltage technique with fixed capacitor arrangement, double-phase lock-in amplifier (Elektron-Manufaktur Mahlsdorf, Germany), high impedance buffer of 20 Gohm, 100 W halogen light source, and quartz prizm monochromator (Bausch & Lomb).

3. Results and discussion

We prepared $MAPbI_3$ films under five different vapor ambiences *e.g.* N_2, GBL/N_2, DMSO/N_2, DMF/N_2, and perovskite precursors (PbI_2+MAI+GBL+DMSO)/N_2 ambiences. The same N_2 flow was constantly applied in all conditions to reduce humidity effects. The $MAPbI_3$ film morphology was examined using scanning electron microscopy (SEM) (Fig. 1b). The images revealed drastic shifts in morphology under the influences of different chemical vapors; only two conditions i.e. control with only N_2 and perovskite precursor ambience with N_2 showed typical flat surfaces with dark brown colors (Fig. 1b inset). We hypothesized that as some solvents (i.e. DMSO and DMF) could from intermediate states with PbI_2 and MAI [25, 26], the crystallization process was disturbed. Optically, $MAPbI_3$ films under DMSO/N_2 and DMF/N_2 vapor ambiences were pale brown. Films under GBL/N_2 and PE/N_2 ambiences

consistently processed small pinholes throughout the top surfaces. In agreement with the microscopy results, films formed under DMSO/N_2 and DMF/N_2 showed little absorption (Fig. 1c) The other three films showed typical absorption of 3D $MAPbI_3$ with the onset around 780 nm [27].

As vapor contaminations especially from perovskite precursors used in prior batch of production represent likely threats for perovskite manufacturing, we developed a prolonged 1-step deposition technique or repeated cation doping (RCD) to alleviate such issues. RCD is a prolong doping of methyl ammonium cation after the typical one step fabrication in hope to prolong crystallization process and enhance crystallinity while resetting any morphology distortion from vapor contaminations. To find the optimal conditions of methyl ammonium cation doping, many parameters including solvent types, solvent amount, timing, dropping rate, spinning protocols, and heat treatment were carefully optimized.

The effect of dropping rate was shown in figure 2 where we varied the intervals between MAI dropping onto MAI/DMSO/PbI_2 intermediate phases on top of the TiO_2 layer using 10 second, 5 second, and 3 second intervals, respectively. The morphology showed polygon-grain feather, more compact formation, and less pin-holes with increasing rate of dropping (Fig 2a). As a result, RCD with the 3 second interval was mainly used in this study.

To apply the RCD technique under chemical vapor ambiences, a TiO_2 substrate was left in the spinner chamber while introducing each chemical vapor ambience (*e.g.* GBL/N_2, DMSO/N_2, DMF/N_2 and PE precursors/N_2). Later on, typical 1-step film fabrication was subsequently applied with the optimized RCD protocol all under the vapor influence. With RCD, the $MAPbI_3$ films (Fig. 2b) showed much improvement in terms of smoothness, coverage, and a number of pinholes even when fabricated in DMSO/N_2 and DMF/N_2 vapor ambiences. Optical images along with absorption spectra further corroborated (Fig. 2c and 2d) the benefits of RCD in all vapor ambiences.

With RCD, all UV absorption spectra showed strong band-edge at ~780 nm, indicating that the resulting films still have the usual 3D $MAPbI_3$ structure. With increasing rate of MA^+ dropping from the 10 second interval to the 3 second interval, increased absorbance in the range of 780 – 900 nm and reduced absorbance in the range of 300 – 500 nm (flat region) were observed. This phenomenon was reported to be more scattering from microcrystal perovskites yet less scattering from nanometer-sized perovskite crystals[24], further demonstrating high film quality with RCD. The flat feature between 300 nm and 500 nm also represents bulk and $MAPbI_3$ single crystalline-like characteristics[28]. Interestingly, UV-Visible absorption spectra of the $MAPbI_3$ films that were fabricated in chemical vapor ambiences showed similar promising features except for RCD under the DMSO/N_2 or DMF/N_2 condition. Nevertheless, RCD (DMSO/N_2 or DMF/N_2) did have improved coverage and absorbance. As both DMSO and DMF could form intermediate states with MAI and PbI_2 i.e. MAI-DMSO-PbI_2 and MAI-DMF-PbI_2[25, 26], under the saturated DMSO or DMF ambience, MAI-DMSO-PbI_2 or MAI-DMF-PbI_2 might remain under such intermediate states perpetually, retarding growth of perovskite and causing RCD less effective.

To identify the phase composition and crystallinity of $MAPbI_3$, the films were examined by the X-ray diffraction (XRD) as shown in Fig. 2e. RCD intensified XRD peaks 5 times or more at all key perovskite positions i.e. (110), (220), and (310) using identical XRD settings under most vapor conditions, further establishing RCD-enhanced crystallinity. Only little to no PbI_2 was found after RCD. These XRD results resonate with the UV-visible results discussed earlier. With RCD, perovskites experience extended crystallization process, leading to slower formation and better crystallinity.

To study charge separation ability and trap states, the $MAPbI_3$ films were prepared on FTO substrate for characterizing by surface photovoltage technique (SPV) as described intensively in previous publications [29–31]. SPV results are shown in Fig.3. The black line represents in-phase signals or fast responses, while the red line represents out-of-phase signals or slow responses. The data showed the typical perovskite onset at 1.5 eV and the PbI_2 peak (if any) around 2.3 eV, as previously demonstrated by Supasai *et. al*. The negative signals of both fast and slow responses depict p-type in the depletion region (electron moving away from FTO) [29] and two mechanisms of charge separation in perovskite [31] . With RCD application, SPV signals (proportional to amount of excited charge x charge separation distance) were increased, demonstrating better charge separation. At same time, PbI_2 traces at 2.3 eV disappeared with application of RCD. Furthermore, the characteristic energies of tail defect states (E_t) were consistently lessen after applying RCD (as shown in table 1), demonstrating less disorder resulted from electronic states. RCD with the 3 sec interval had the lowest defect energies. More details on E_t calculations can be found in the supplementary information. However, RCD is less effectively for $DMSO/N_2$ and DMF/N_2 ambiences, in agreement with other measurements. We believe with higher crystallinity, there are fewer boundary trap states and therefore better electronic properties.

Lastly, we explored the potentials of RCD to recover wasted perovskite films where perovskite had already converted back to PbI_2. Wasted films were prepared by heating usable perovskite films at 300 $^{\circ}$C for 3 minutes; all top surfaces became yellow. The wasted films were then introduced with RCD under N_2 ambience. RCD using higher MAI amount (full doping) had more potentials to freshen wasted films as absorption results indicated more bulk-like characteristics (Fig. 4b). RCD using both MAI amounts did lead to morphology improvement and good charge separation (Fig. 4a and 4c). However, as wasted films originally had very large pinholes, RCD merged smaller grains together, creating more compact perovskite islands and leaving large empty areas in between. Little PbI_2 still remained (as shown in Fig 4c around 2.3 eV in comparison to the control sample). This procedure could be further studied and optimized for future recycling process.

4. Conclusion

In this work, we investigated the negative effects of chemical vapor ambiences on perovskite formation and developed a new versatile technique called RCD to help generate thin films with smoother morphology, more compact grain formation, and less pin-holes under various environments. RCD promotes higher crystallinity, more charge separation, and less tail defects under most ambient conditions. RCD is a useful tool, improving normal perovskites, perovskites under chemical vapors, and wasted perovskites.

List of abbreviations

RCD : repeated cation doping

Acknowledgments

This work was mainly supported by Thailand Research Fund (MRG59-Pongsakorn Kanjanaboos). We acknowledge Faculty of Science, Mahidol University and DPST research fund. We thank EGAT & NSTDA (funding number# FDA-CO-2560-5449-TH) for facility support. We acknowledge Dr. Thidarat Supasai from Department of Materials Science, Kasetsart University for providing access to and expertise on all SPV experiments. We acknowledge Atittaya Naikaew for optimizing the standard sample protocol and Zoubeir Saraw for helping with the wasted perovskite experiment. We acknowledge Nakorn Henjongchom for helping with SPV and XRD experiments. We thank Dr. Pasit Pakawatpanurut, Paphada Kaewurai, and Koth Amratisha for fruitful discussions.

References

1. Manser JS, Christians JA, Kamat P V. (2016) Intriguing Optoelectronic Properties of Metal Halide Perovskites. Chem Rev 116:12956–13008 . doi: 10.1021/acs.chemrev.6b00136

2. Aygüler MF, Weber MD, Puscher BMD, et al (2015) Light-Emitting Electrochemical Cells Based on Hybrid Lead Halide Perovskite Nanoparticles. J Phys Chem C 150415033719003 . doi: 10.1021/acs.jpcc.5b02959

3. Yuan M, Quan LN, Comin R, et al (2016) Perovskite energy funnels for efficient light-emitting diodes. Nat Nanotechnol 1–27 . doi: 10.1038/nnano.2016.110

4. Luo S, Daoud W a (2015) Recent progress in organic – inorganic halide perovskite solar cells : mechanisms and material. J Mater Chem A 3:8992–9010 . doi: 10.1039/c4ta04953e

5. Gonzalez-Pedro V, Juarez-Perez EJ, Arsyad WS, et al (2014) General working principles of CH3NH3PbX3 perovskite solar cells. Nano Lett 14:888–893 . doi: 10.1021/nl404252e

6. Song Z, Watthage SC, Phillips AB, Heben MJ (2016) Pathways toward high-performance perovskite solar cells: review of recent advances in organo-metal halide perovskites for photovoltaic applications. J Photonics Energy 6:22001 . doi: 10.1117/1.JPE.6.022001

7. Wang G, Liu D, Xiang J, et al (2016) Efficient perovskite solar cell fabricated in ambient air using one-step spin-coating. RSC Adv 6:43299–43303 . doi: 10.1039/C6RA05893K

8. Heo JH, Lee MH, Jang MH, Im SH (2016) Highly efficient $CH_3NH_3PbI_{3-x}Cl_x$ mixed halide perovskite solar cells prepared by re-dissolution and crystal grain growth via spray coating. J Mater Chem A 4:17636–17642 . doi: 10.1039/C6TA06718B

9. Zheng E, Wang XF, Song J, et al (2015) PbI<inf>2</inf>-Based Dipping-Controlled Material Conversion for Compact Layer Free Perovskite Solar Cells. ACS Appl Mater Interfaces 7:18156–18162 . doi: 10.1021/acsami.5b05787

10. Xing G, Mathews N, Lim SS, et al (2014) Low-temperature solution-processed

wavelength-tunable perovskites for lasing. Nat Mater 13:476–80 . doi: 10.1038/nmat3911

11. Ball JM, Lee MM, Hey A, Snaith HJ (2013) Low-temperature processed meso-superstructured to thin-film perovskite solar cells. Energy Environ Sci 6:1739 . doi: 10.1039/c3ee40810h

12. Lee H, Kim A, Kwon HC, et al (2016) Retarding Crystallization during Facile Single Coating of NaCl-Incorporated Precursor Solution for Efficient Large-Area Uniform Perovskite Solar Cells. ACS Appl Mater Interfaces 8:29419–29426 . doi: 10.1021/acsami.6b08783

13. Kim BJ, Kim DH, Kwon SL, et al (2016) Selective dissolution of halide perovskites as a step towards recycling solar cells. Nat Commun 7:11735 . doi: 10.1038/ncomms11735

14. Jeon NJ, Noh JH, Kim YC, et al (2014) Solvent engineering for high-performance inorganic–organic hybrid perovskite solar cells. Nat Mater 13:897–903 . doi: 10.1038/nmat4014

15. Ji L, Zhang T, Wang Y, et al (2017) Realizing Full Coverage of Stable Perovskite Film by Modified Anti-Solvent Process. Nanoscale Res Lett 12: . doi: 10.1186/s11671-017-2117-6

16. Nie W, Tsai H, Asadpour R, et al (2015) High-efficiency solution-processed perovskite solar cells with millimeter-scale grains. Science (80-) 347:522–525 . doi: 10.1126/science.aaa0472

17. Aguiar JA, Wozny S, Alkurd NR, et al (2016) Effect of Water Vapor, Temperature, and Rapid Annealing on Formamidinium Lead Triiodide Perovskite Crystallization. ACS Energy Lett 1:155–161 . doi: 10.1021/acsenergylett.6b00042

18. Shaikh JS, Shaikh NS, Sheikh AD, et al (2017) Perovskite solar cells: In pursuit of efficiency and stability. Mater Des 136:54–80 . doi: 10.1016/j.matdes.2017.09.037

19. Kim HS, Lee CR, Im JH, et al (2012) Lead iodide perovskite sensitized all-solid-state submicron thin film mesoscopic solar cell with efficiency exceeding 9%. Sci Rep 2:1–7 . doi: 10.1038/srep00591

20. Park BS, Lee S, Yoon S, et al (2018) Methylammonium lead mixed halide films processed with a new composition for planar perovskite solar cells. Appl Surf Sci 427:421–426 . doi: 10.1016/j.apsusc.2017.08.212

21. Burschka J, Pellet N, Moon S-J, et al (2013) Sequential deposition as a route to high-performance perovskite-sensitized solar cells. Nature 499:316–320 . doi: 10.1038/nature12340

22. Xiao Z, Bi C, Shao Y, et al (2014) Efficient, high yield perovskite photovoltaic devices grown by interdiffusion of solution-processed precursor stacking layers. Energy Environ Sci 7:2619–2623 . doi: 10.1039/C4EE01138D

23. Ruankham P, Wongratanaphisan D, Gardchareon A, et al (2017) Full coverage of perovskite layer onto ZnO nanorods via a modified sequential two-step deposition method for efficiency enhancement in perovskite solar cells. Appl Surf Sci 410:393–400 . doi: 10.1016/j.apsusc.2017.03.096

24. Mokhtar MZ, Chen M, Whittaker E, et al (2017) $CH_3NH_3PbI_3$ films prepared by combining 1- and 2-step deposition: how crystal growth conditions affect properties. Phys Chem Chem Phys 19:7204–7214 . doi: 10.1039/C7CP00471K

25. Huang P-H, Wang Y-H, Ke J-C, Huang C-J (2017) The Effect of Solvents on the

Performance of CH3NH3PbI3 Perovskite Solar Cells. Energies 10:599 . doi: 10.3390/en10050599

26. Xie L, Hwang H, Kim M, Kim K (2017) Ternary solvent for CH 3 NH 3 PbI 3 perovskite films with uniform domain size. Phys Chem Chem Phys 19:1143–1150 . doi: 10.1039/C6CP06709C

27. Ma C, Leng C, Ji Y, et al (2016) 2D/3D perovskite hybrids as moisture-tolerant and efficient light absorbers for solar cells. Nanoscale 8:18309–18314 . doi: 10.1039/C6NR04741F

28. Jain SM, Philippe B, Johansson EMJ, et al (2016) Vapor phase conversion of PbI_2 to $CH_3NH_3PbI_3$: spectroscopic evidence for formation of an intermediate phase. J Mater Chem A 4:2630–2642 . doi: 10.1039/C5TA08745G

29. Supasai T, Rujisamphan N, Ullrich K, et al (2013) Formation of a passivating CH3NH3PbI 3/PbI2 interface during moderate heating of CH 3NH3PbI3 layers. Appl Phys Lett 103: . doi: 10.1063/1.4826116

30. Juma AO, Azarpira A, Steigert A, et al (2013) Role of chlorine in In2S3 for band alignment at nanoporous-TiO2/In2S3 interfaces Role of chlorine in In 2 S 3 for band alignment at nanoporous-TiO 2 /In 2 S 3 interfaces. J Appl Phys Addit Inf J Appl Phys J Homepage 114:2–7 . doi: 10.1063/1.4817766doi.org/10.1063/1.4817766

31. Prajongtat P, Dittrich T (2015) Precipitation of $CH_3NH_3PbCl_3$ in $CH_3NH_3PbI_3$ and Its Impact on Modulated Charge Separation. J Phys Chem C 119:9926–9933 . doi: 10.1021/acs.jpcc.5b01667

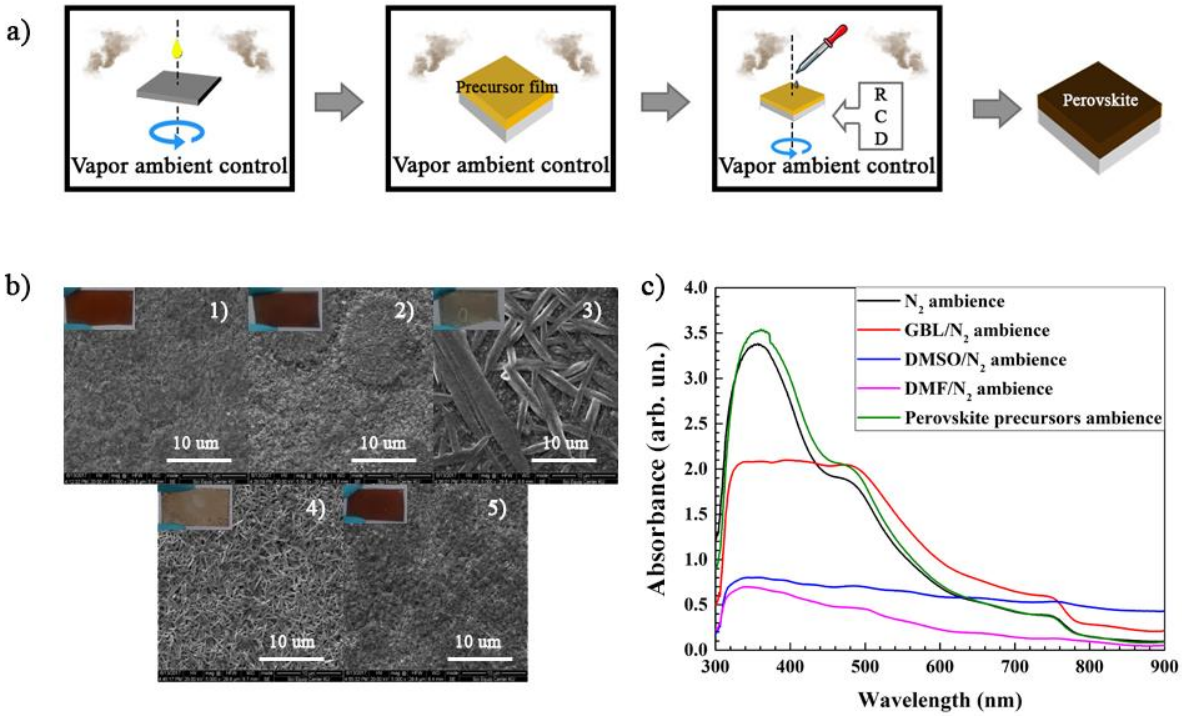

Figure 1: (a) Diagram of repeated cation doping (RCD) method. (b) SEM images of perovskite films formed under N_2, GBL/N_2, DMSO/N_2, DMF/N_2, and perovskite precursors/N_2 ambiences respectively with optical images as insets. (c) Absorption spectra of perovskite films.

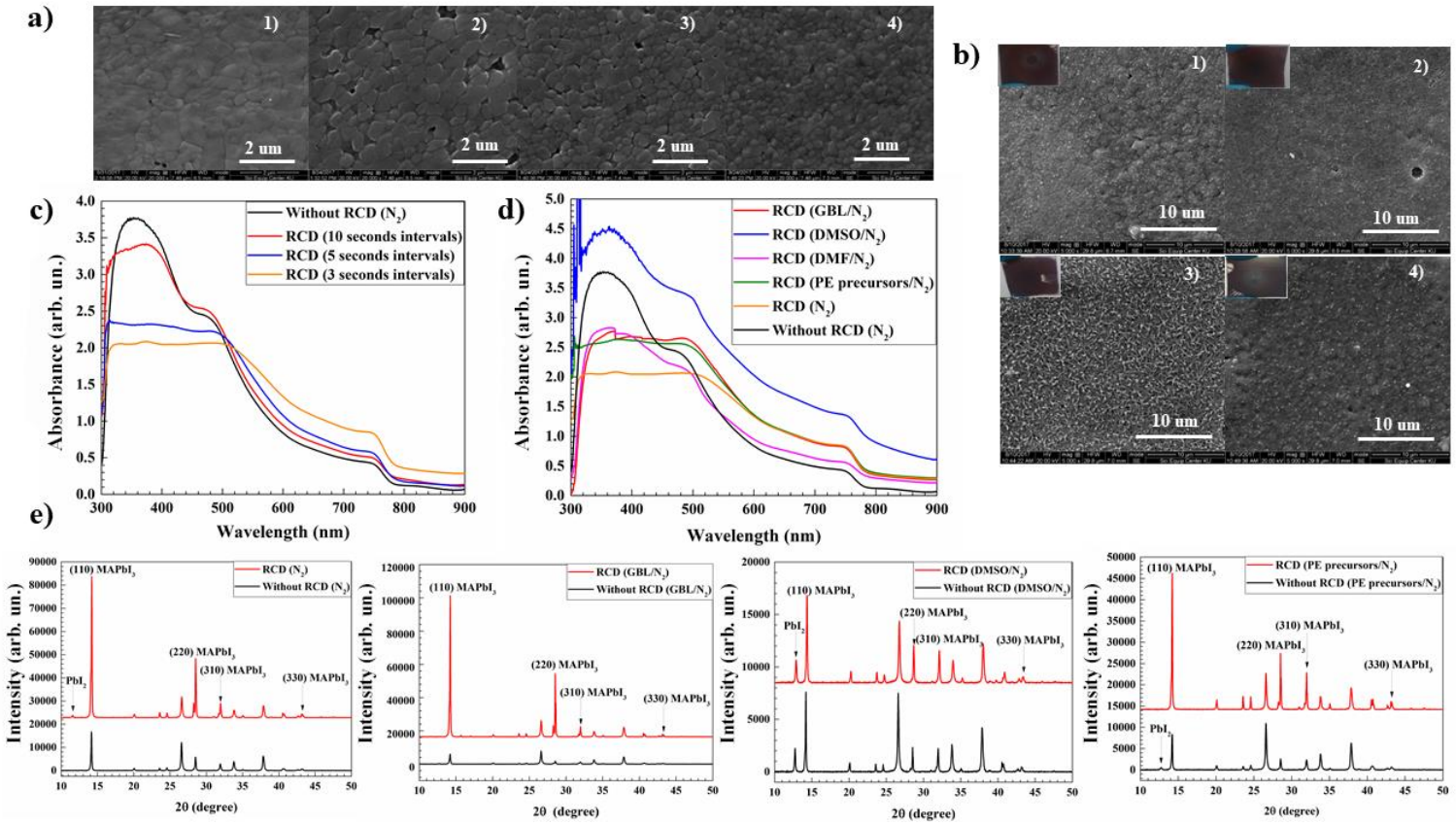

Figure 2: (a) SEM images of perovskite film in N_2 ambience without RCD and with RCD using 10 second, 5 second, and 3 second intervals, respectively. (b) SEM images of perovskite films with RCD using 3 second interval in GBL/N_2, DMSO/N_2, DMF/N_2, and PE precursors/N_2 ambiences. (c) Absorption spectra of perovskite films with RCD using 10 s, 5 s, and 3 s intervals. (d) Absorption spectra of perovskite films with RCD using 3 seconds interval in N_2, GBL/N_2, DMSO/N_2, DMF/N_2, and Perovskite precursors/N_2 ambiences. (e) XRD of perovskite film with and without RCD on TiO_2/FTO.

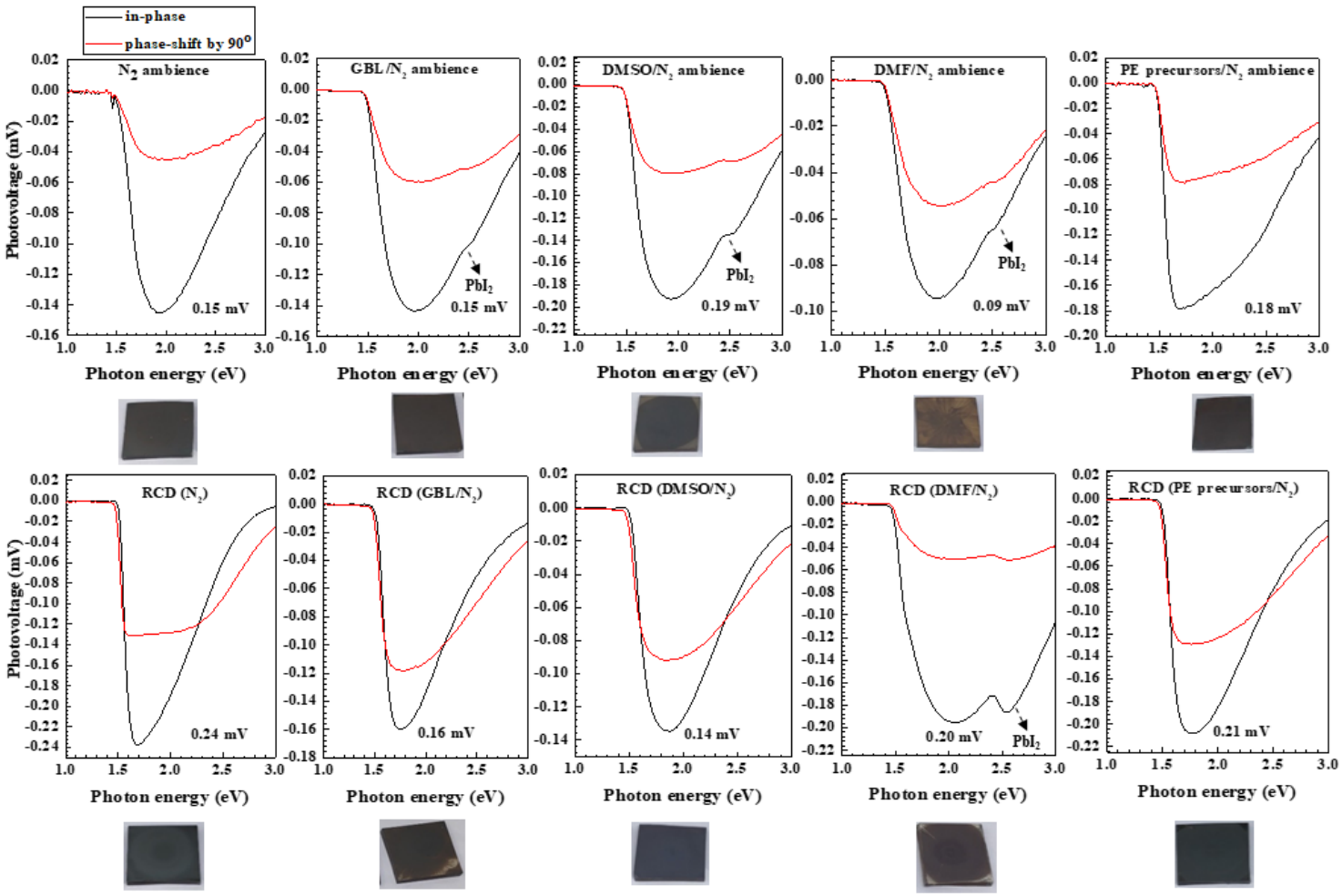

Figure 3: SPV spectra of perovskite films in ambiences from left to right; N_2, GBL/N_2, DMSO/N_2, DMF/N_2, and Perovskite precursors/N_2. Upper row: without RCD; lower row: with RCD.

AMBIENCE	W-W/O RCD	E_t (meV)
N_2	W/O RCD	23
	RCD – 10 sec intervals	21
	RCD – 5 sec intervals	22
	RCD – 3 sec intervals	17
GBL/N_2	W/O RCD	27
	RCD – 3 sec intervals	23
DMSO/N_2	W/O RCD	21
	RCD – 3 sec intervals	22
DMF/N_2	W/O RCD	24
	RCD – 3 sec intervals	25
PE PRECURSORS/N_2	W/O RCD	21
	RCD – 3 sec intervals	21

Table 1: The characteristic energies of tail defect state (E_t) measurements for perovskite films in ambiences without RCD and with RCD. The fitting and calculation were shown in the supplementary information.

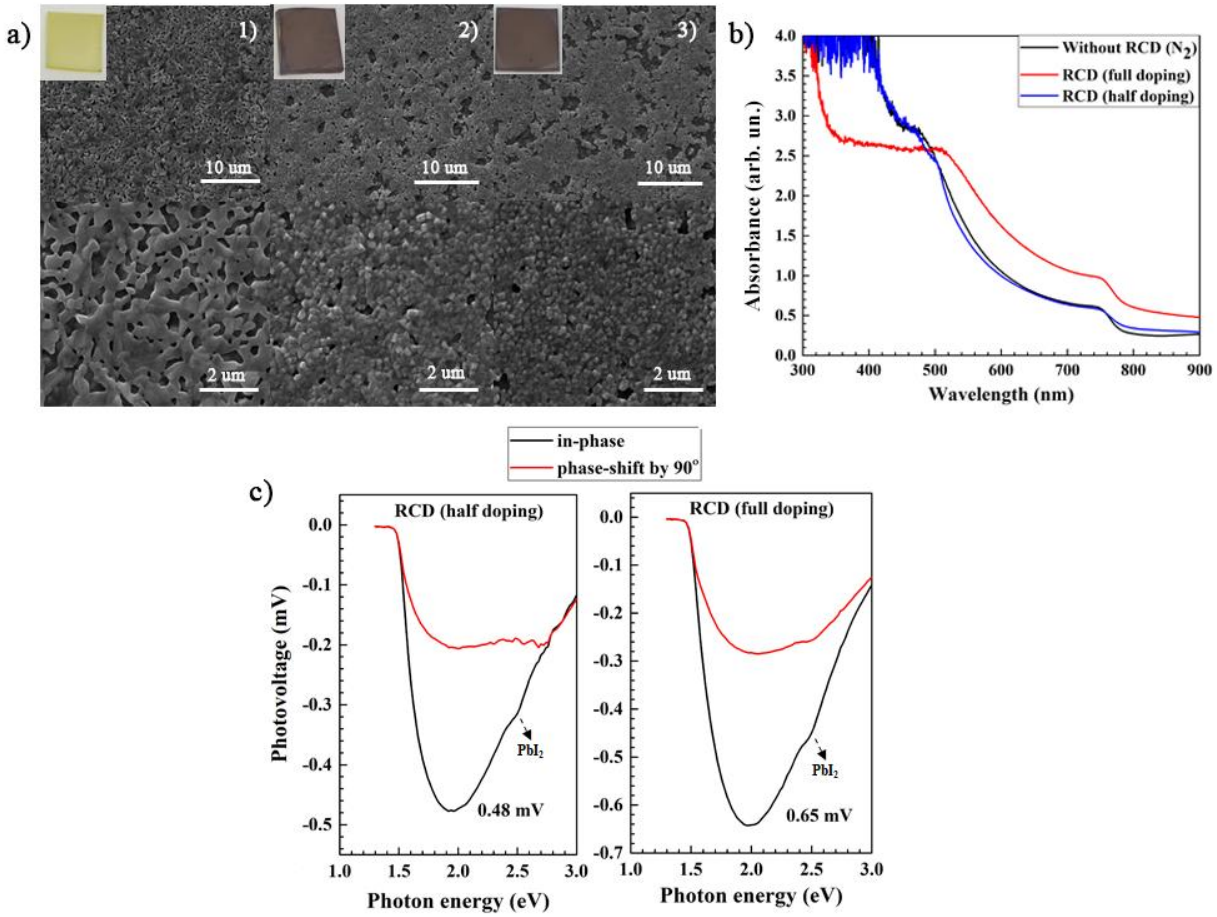

Figure 4: (a) SEM of wasted perovskite films (left) and recycled perovskite films with RCD using half doping (middle) and full doping (right) (b) Absorption spectra of recycled perovskite films. The black line is a regular perovskite control sample for comparison. (c) SPV spectra of recycled perovskite films.

5. **Appendix**

Accepted manuscript

Reconditioning Perovskite films under Vapor Environments through Repeated Cation Doping

Chirapa Boonthum[1], Kusuma Pinsuwan[1], Jitprabhat Ponchai[1], Toemsak Srikhirin[1,2], Pongsakorn Kanjanaboos[1,3]*

[1] *School of Materials Science and Innovation, Faculty of Science, Mahidol University, Bangkok, Thailand 10400*

[2] *Department of Physics, Faculty of Science, Mahidol University, Bangkok, Thailand 10400*

[3] *Center of Excellence for Innovation in Chemistry (PERCH-CIC), Office of Higher Education Commission, Ministry of Education (OHEC)*

**corresponding author Email : Pongsakorn.kan@mahidol.ac.th*

Abstract

Perovskites have attracted considerable attention for application as high-efficiency photovoltaic devices due to their low-cost and low-temperature fabrication. Good surface and high crystallinity are necessary for high-performance devices. We examine the negative effects of chemical ambiences on perovskite crystal formation and morphology. The repeated cation doping (RCD) technique was developed to remedy the issues by gradually dropping methyammonium ions on top of about-to-formed perovskite surfaces to cause recrystallization. RCD promotes pinhole-free, compact, and polygonal-like surfaces under various vapor conditions. Furthermore, electronic properties and crystallization are enhanced. RCD extends its benefits beyond perovskites under vapor ambiences, improving regular and wasted perovskites.

Keywords: Perovskite; Perovskite Formation; Crystallization; Ambient Effects; Repeated Cation Doping (RCD); Recycled Perovskite; Fabrication Process

The organic-inorganic perovskite materials have been popular these days because of their excellent semiconductor behaviors coupled with low cost fabrication processes[1]. These hybrid materials have great potentials for modern electronic devices such as Light-Emitting Electrochemical Cells (LECs)[2], Light-Emitting diodes (LEDs)[3] and solar cells[4,5], having outstanding characteristics i.e. direct bandgap, high charge-carrier mobility, low trap density of electron, and high absorption coefficient[6]. Unlike silicon-based solar cells, these materials can be fabricated through facile processing e.g. spin-coating[7], spray coating[8], sputter coating[9] and dip-coating[10]. Moreover, perovskite can be expediently prepared from abundant chemical substances and fabricated in low-temperature production[11,12].

As high power conversion efficiency (PCE) necessitates good morphology and electronic properties, a lot of previous studies have focused on improving perovskite layer through various methods e.g., NaCl-incorporated precursor solution[13], MABr-selective Ostwald ripening process[14], anti-solvent engineering[15,16], and solvent annealing process[17]. During and after perovskite film formation, perovskite properties are highly sensitive toward surrounding ambient conditions and fabrication protocols[18,19]. To ensure the success of future large-scale perovskite production, effects of different precursor vapors (i.e. possible leftovers or contaminations) on perovskite morphology and formation are studied in this work. Here, we introduced various potential vapors including gamma-butyrolactone (GBL), dimethyl sulfoxide (DMSO), *N*,*N*-dimethylformamide (DMF) and mixed perovskite precursor vapors (PE) (in 7:3 GBL:DMSO) inside a sealed spinner system during perovskite formation. Film morphology was significantly altered for different vapor ambiences; however, consistent features were observed under repeated trials for the same vapors. Many undesirable features such as pinholes, nonhomogeneousness, and roughness were seen. To overcome this issue, we developed repeated cation doping (RCD) method which slowly drops extra salt mixture such as Methyl ammonium Iodide (MAI) over a fixed period of time on top of about-to-formed perovskite layers to cause gradual recrystallization to improve the perovskite layer. This new technique is a prolonged 1-step deposition unlike the traditional 1-step technique[7,15,20,21], the 2-step technique[22–24], or the combination of 1-step and 2-step techniques[25].

Perovskite ($MAPbI_3$) film was fabricated on top of compact TiO_2/ fluorine doped tin oxide. 1.5 M precursor solution was prepared by mixing equimolar ratio of lead iodide (PbI_2) and methyl ammonium iodide (MAI) in g-butyrolactone (GBL, Sigma-Aldrich)/dimethyl sulfoxide (DMSO, Sigma-Aldrich); 7/3 v/v and stirred at 70 °C for 30 minutes. The perovskite solution was then filtered with a PTFE syringe filter (Whatman, 0.22 um) and spin-coated on a compact TiO_2/ fluorine doped tin oxide substrate. The substrate was spun in a two-speed protocol at 500 rpm for 10 seconds (acceleration of 250 rpm /second) and then 5000 RPM for 60 seconds (acceleration of 1500 rpm /second), followed by toluene dripping[15] at the 30th second. For the spinning protocol, N_2 was continuously flowing at a fixed rate of $\sim 5x10^{-6}$ cubic meters per second. The perovskite film was fully crystallized by annealing at 100 °C for 15 minutes on a hotplate.

For the chemical vapor ambient study, the saturated vapor environment was created by filling the bottom halve of the closed spinner chamber with kimwipes excessively soaked with a desired solvent (~ 50 ml). The chamber size is 0.2 m (diameter) x 0.14 m (height). The compact TiO_2/ fluorine doped tin oxide substrate was first left in a closed spinner chamber that maintained specific saturated solvent vapor for 8 minutes before the $MAPbI_3$ film was prepared under the vapor environment using the two speed protocol. N_2 was always flowing at a fixed rate of ~ $5x10^{-6}$ cubic meters per second.

The repeated cation doping technique (RCD) had the same initial protocols as regular and vapor processes. However, additional cation droppings (3, 6, or 10 times) were carefully implemented to cause gradual re-crystallization. Specifically, the substrate was spun in a two-speed protocol at 500 rpm for 10 seconds and then 5000 RPM for 60 seconds. The one-step perovskite solution was dropped on substrate before the first speed protocol as usual. 3 mL of 0.05 M MAI in ethanol/isopropanol (1/1 v/v) was gradually dropped on top of the about-to-formed perovskite layer every 3 seconds for 30 seconds (10 times of dropping) during the second speed protocol through a syringe, followed by toluene dripping at the 33th second. The perovskite film was then annealed at 100 °C for 15 minutes. For RCD with 10 second and 5 second intervals, the same procedure was applied; however, the time intervals between consecutive MAI droppings were 10 seconds (total 3 times of dropping) and 5 seconds (6 times), respectively.

A wasted film was prepared by heating perovskite film at 300 °C for 5 minutes and then rested in air to cool down to room temperature. The film was fully changed to the yellowish state. For full doping, 7.8 ml of 0.05 M MAI in ethanol/isopropanol (1/1 v/v) was gradually dropped on top of the wasted film every 3 seconds for 78 seconds (total 26 times of dropping) under the second spinning protocol of 5000 rpm for 106 seconds, followed by toluene dripping at 81th second. For the half doping protocol, the MAI solution has the same concentration but with reduced amount of 3.9 ml.

Lead iodide (PbI2, 99.95% purity), dimethyl sulfoxide (DMSO, anhydrous grade), g-butyrolactone (GBL, anhydrous grade), N,N-dimethylformamide (DMF, anhydrous grade), Isopropanol (IPA, anhydrous grade) were all purchased from Sigma-Aldrich. Ethanol (anhydrous grade), toluene (anhydrous grade), and methyl ammonium iodide (MAI) were purchased from Fisher Scientific, Kanto chemical, and Dyesol, respectively.

The perovskite film morphologies were observed using an scanning electron microscope (Quanta 450 FEI, Tungsten filament electron source, 20 kV, secondary electron (SE) mode). Absorption spectra were achieved using a uv-vis spectrophotometer (Shimadzu UV-2600, Deuterium lamp light source, double–beam, 1 nm slit width, absorbance mode). X-ray diffraction was performed using a X-ray diffractometer (Advance Bruker, Cu Kα radiation, LYNXEYE high-resolution energy-dispersive 1-D detector, detector scan mode with step size of 0.020449 degree, 0.8 s per step, and theta start of 5.00 degree). The surface photovoltage signals were obtained through a modulated surface photovoltage technique with fixed capacitor arrangement, double-phase lock-in amplifier (Elektron-Manufaktur Mahlsdorf,

Germany), high impedance buffer of 20 Gohm, 100 W halogen light source, and quartz prizm monochromator (Bausch & Lomb).

We prepared $MAPbI_3$ films under five different vapor ambiences *e.g.* N_2, GBL/N_2, DMSO/N_2, DMF/N_2, and perovskite precursors (PbI_2+MAI+GBL+DMSO)/N_2 ambiences. The same N_2 flow was constantly applied in all conditions to reduce humidity effects. The $MAPbI_3$ film morphology was examined using scanning electron microscopy (SEM) (Fig. 1b). The images revealed drastic shifts in morphology under the influences of different chemical vapors; only two conditions i.e. control with only N_2 and perovskite precursor ambience with N_2 showed typical flat surfaces with dark brown colors (Fig. 1b inset). We hypothesized that as some solvents (i.e. DMSO and DMF) could from intermediate states with PbI_2 and MAI [26,27], the crystallization process was disturbed. Optically, $MAPbI_3$ films under DMSO/N_2 and DMF/N_2 vapor ambiences were pale brown. Films under GBL/N_2 and PE/N_2 ambiences consistently processed small pinholes throughout the top surfaces. In agreement with the microscopy results, films formed under DMSO/N_2 and DMF/N_2 showed little absorption (Fig. 1c) The other three films showed typical absorption of 3D $MAPbI_3$ with the onset around 780 nm [28].

As vapor contaminations especially from perovskite precursors used in prior batch of production represent likely threats for perovskite manufacturing, we developed a prolonged 1-step deposition technique or repeated cation doping (RCD) to alleviate such issues. RCD is a prolong doping of methyl ammonium cation after the typical one step fabrication in hope to prolong crystallization process and enhance crystallinity while resetting any morphology distortion from vapor contaminations. To find the optimal conditions of methyl ammonium cation doping, many parameters including solvent types, solvent amount, timing, dropping rate, spinning protocols, and heat treatment were carefully optimized.

The effect of dropping rate was shown in figure 2 where we varied the intervals between MAI dropping onto MAI/DMSO/PbI_2 intermediate phases on top of the TiO_2 layer using 10 second, 5 second, and 3 second intervals, respectively. The morphology showed polygon-grain feather, more compact formation, and less pin-holes with increasing rate of dropping (Fig 2a). As a result, RCD with the 3 second interval was mainly used in this study.

To apply the RCD technique under chemical vapor ambiences, a TiO_2 substrate was left in the spinner chamber while introducing each chemical vapor ambience (*e.g.* GBL/N_2, DMSO/N_2, DMF/N_2 and PE precursors/N_2). Later on, typical 1-step film fabrication was subsequently applied with the optimized RCD protocol all under the vapor influence. With RCD, the $MAPbI_3$ films (Fig. 2b) showed much improvement in terms of smoothness, coverage, and a number of pinholes even when fabricated in DMSO/N_2 and DMF/N_2 vapor ambiences. Optical images along with absorption spectra further corroborated (Fig. 2c and 2d) the benefits of RCD in all vapor ambiences.

With RCD, all absorption spectra showed strong band-edge at ~780 nm, indicating that the resulting films still have the usual 3D $MAPbI_3$ structure. With increasing rate of MA^+ dropping from the 10 second interval to the 3 second interval, increased absorbance in the range of 780 – 900 nm and reduced absorbance in the range of 300

– 500 nm (flat region) were observed. This phenomenon was reported to be more scattering from microcrystal perovskites yet less scattering from nanometer-sized perovskite crystals[25], further demonstrating high film quality with RCD. The flat feature between 300 nm and 500 nm also represents bulk and $MAPbI_3$ single crystalline-like characteristics[29]. Interestingly, the absorption spectra of the $MAPbI_3$ films that were fabricated in chemical vapor ambiences showed similar promising features except for RCD under the $DMSO/N_2$ or DMF/N_2 condition. Nevertheless, RCD ($DMSO/N_2$ or DMF/N_2) did have improved coverage and absorbance. As both DMSO and DMF could form intermediate states with MAI and PbI_2 i.e. MAI-DMSO-PbI_2 and MAI-DMF-PbI_2[26,27], under the saturated DMSO or DMF ambience, MAI-DMSO-PbI_2 or MAI-DMF-PbI_2 might remain under such intermediate states perpetually, retarding growth of perovskite and causing RCD less effective.

To identify the phase composition and crystallinity of $MAPbI_3$, the films were examined by the X-ray diffraction (XRD) as shown in Fig. 2e. RCD intensified XRD peaks 5 times or more at all key perovskite positions i.e. (110), (220), and (310) using identical XRD settings under most vapor conditions, further establishing RCD-enhanced crystallinity. Only little to no PbI_2 was found after RCD. These XRD results resonate with the UV-visible results discussed earlier. With RCD, perovskites experience extended crystallization process, leading to slower formation and better crystallinity.

To study charge separation ability and trap states, the $MAPbI_3$ films were prepared on FTO substrate for characterizing by surface photovoltage technique (SPV) as described intensively in previous publications [30–32]. SPV results are shown in Fig.3. The black line represents in-phase signals or fast responses, while the red line represents out-of-phase signals or slow responses. The data showed the typical perovskite onset at 1.5 eV and the PbI_2 peak (if any) around 2.3 eV, as previously demonstrated by Supasai *et. al*. The negative signals of both fast and slow responses depict p-type in the depletion region (electron moving away from FTO) [30] and two mechanisms of charge separation in perovskite [32] . With RCD application, SPV signals (proportional to amount of excited charge x charge separation distance) were increased, demonstrating better charge separation. At same time, PbI_2 traces at 2.3 eV disappeared with application of RCD. Furthermore, the characteristic energies of tail defect states (E_t) were consistently lessen after applying RCD (as shown in table 1), demonstrating less disorder resulted from electronic states. RCD with the 3 sec interval had the lowest defect energies. More details on E_t calculations can be found in the supplementary information. However, RCD is less effectively for $DMSO/N_2$ and DMF/N_2 ambiences, in agreement with other measurements. We believe with higher crystallinity, there are fewer boundary trap states and therefore better electronic properties.

To reduce toxic wastes like Pb, perovskites should be recycled. Jena *et at.* demonstrated the reconversion of PbI_2 through reapplying MAI solution one time similar to a two-step deposition, studying temperature effects on the performance of recycled perovskites[33]. In this work, we explored the potentials of RCD by applying cations repeatedly (13 times or 26 times) to cause gradual recrystallization and recover wasted perovskite films where perovskite had already converted back to PbI_2. Wasted films were prepared by heating usable perovskite films at 300 ℃ for 3

minutes; all top surfaces became yellow. The wasted films were then introduced with RCD under N_2 ambience. RCD using higher MAI amount (full doping) had more potentials to freshen wasted films as absorption results indicated more bulk-like characteristics (Fig. 4b). RCD using both MAI amounts did lead to morphology improvement and good charge separation (Fig. 4a and 4c). However, as wasted films originally had very large pinholes, RCD merged smaller grains together, creating more compact perovskite islands and leaving large empty areas in between. Little PbI_2 still remained (as shown in Fig 4c around 2.3 eV in comparison to the control sample). This procedure could be further studied and optimized for future recycling process.

In this work, we investigated the negative effects of chemical vapor ambiences on perovskite formation and developed a new versatile technique called RCD to help generate thin films with smoother morphology, more compact grain formation, and less pin-holes under various environments. RCD promotes higher crystallinity, more charge separation, and less tail defects under most ambient conditions. RCD is a useful tool, improving normal perovskites, perovskites under chemical vapors, and wasted perovskites.

Acknowledgments

This work was mainly supported by Thailand Research Fund (MRG59-Pongsakorn Kanjanaboos). We acknowledge Center of Excellence for Innovation in Chemistry (PERCH-CIC) and Faculty of Science, Mahidol University. We thanks EGAT & NSTDA (funding number# FDA-CO-2560-5449-TH) for facility support. We acknowledge Dr. Thidarat Supasai from Department of Materials Science, Kasetsart University for providing access to and expertise on all SPV experiments. We acknowledge Atittaya Naikaew for optimizing the standard sample protocol and Zoubeir Saraw for helping with the wasted perovskite experiment. We acknowledge Nakorn Henjongchom for helping with SPV and XRD experiments. We thank Dr. Pasit Pakawatpanurut, Paphada Kaewurai, and Koth Amratisha for fruitful discussions.

References

[1] J.S. Manser, J.A. Christians, and P. V. Kamat, Chem. Rev. **116**, 12956 (2016).

[2] M.F. Aygüler, M.D. Weber, B.M.D. Puscher, D.D. Medina, P. Docampo, and R.D. Costa, J. Phys. Chem. C 150415033719003 (2015).

[3] M. Yuan, L.N. Quan, R. Comin, G. Walters, R. Sabatini, O. Voznyy, S. Hoogland, Y. Zhao, E.M. Beauregard, P. Kanjanaboos, Z. Lu, D.H. Kim, and E.H. Sargent, Nat. Nanotechnol. (2016).

[4] S. Luo and W. a Daoud, J. Mater. Chem. A **3**, 8992 (2015).

[5] V. Gonzalez-Pedro, E.J. Juarez-Perez, W.S. Arsyad, E.M. Barea, F. Fabregat-Santiago, I. Mora-Sero, and J. Bisquert, Nano Lett. **14**, 888 (2014).

[6] Z. Song, S.C. Watthage, A.B. Phillips, and M.J. Heben, J. Photonics Energy **6**, 22001 (2016).

[7] G. Wang, D. Liu, J. Xiang, D. Zhou, K. Alameh, B. Ding, and Q. Song, RSC Adv. **6**, 43299 (2016).

[8] J.H. Heo, M.H. Lee, M.H. Jang, and S.H. Im, J. Mater. Chem. A **4**, 17636 (2016).

[9] I. Raifuku, Y. Ishikawa, T. Bourgeteau, Y. Bonnassieux, P. Roca i Cabarrocas, and Y. Uraoka, Appl. Phys. Express **10**, 94101 (2017).

[10] E. Zheng, X.F. Wang, J. Song, L. Yan, W. Tian, and T. Miyasaka, ACS Appl. Mater. Interfaces **7**, 18156 (2015).

[11] G. Xing, N. Mathews, S.S. Lim, N. Yantara, X. Liu, D. Sabba, M. Grätzel, S. Mhaisalkar, and T.C. Sum, Nat. Mater. **13**, 476 (2014).

[12] J.M. Ball, M.M. Lee, A. Hey, and H.J. Snaith, Energy Environ. Sci. **6**, 1739 (2013).

[13] H. Lee, A. Kim, H.C. Kwon, W. Yang, Y. Oh, D. Lee, and J. Moon, ACS Appl. Mater. Interfaces **8**, 29419 (2016).

[14] B.J. Kim, D.H. Kim, S.L. Kwon, S.Y. Park, Z. Li, K. Zhu, and H.S. Jung, Nat. Commun. **7**, 11735 (2016).

[15] N.J. Jeon, J.H. Noh, Y.C. Kim, W.S. Yang, S. Ryu, and S. Il Seok, Nat. Mater. **13**, 897 (2014).

[16] L. Ji, T. Zhang, Y. Wang, P. Zhang, D. Liu, Z. Chen, and S. Li, Nanoscale Res. Lett. **12**, (2017).

[17] W. Nie, H. Tsai, R. Asadpour, A.J. Neukirch, G. Gupta, J.J. Crochet, M. Chhowalla, S. Tretiak, M. a Alam, and H. Wang, Science **347**, 522 (2015).

[18] J.A. Aguiar, S. Wozny, N.R. Alkurd, M. Yang, L. Kovarik, T.G. Holesinger, M. Al-Jassim, K. Zhu, W. Zhou, and J.J. Berry, ACS Energy Lett. **1**, 155 (2016).

[19] J.S. Shaikh, N.S. Shaikh, A.D. Sheikh, S.S. Mali, A.J. Kale, P. Kanjanaboos, C.K. Hong, J.H. Kim, and P.S. Patil, Mater. Des. **136**, 54 (2017).

[20] H.S. Kim, C.R. Lee, J.H. Im, K.B. Lee, T. Moehl, A. Marchioro, S.J. Moon, R. Humphry-Baker, J.H. Yum, J.E. Moser, M. Grätzel, and N.G. Park, Sci. Rep. **2**, 1 (2012).

[21] B.S. Park, S. Lee, S. Yoon, T.J. Ha, and D.W. Kang, Appl. Surf. Sci. **427**, 421 (2018).

[22] J. Burschka, N. Pellet, S.-J. Moon, R. Humphry-Baker, P. Gao, M.K. Nazeeruddin, and M. Grätzel, Nature **499**, 316 (2013).

[23] Z. Xiao, C. Bi, Y. Shao, Q. Dong, Q. Wang, Y. Yuan, C. Wang, Y. Gao, and J. Huang, Energy Environ. Sci. **7**, 2619 (2014).

[24] P. Ruankham, D. Wongratanaphisan, A. Gardchareon, S. Phadungdhitidhada, S. Choopun, and T. Sagawa, Appl. Surf. Sci. **410**, 393 (2017).

[25] M.Z. Mokhtar, M. Chen, E. Whittaker, B. Hamilton, N. Aristidou, S. Ramadan, A. Gholinia, S.A. Haque, P. O'Brien, and B.R. Saunders, Phys. Chem. Chem. Phys. **19**, 7204 (2017).

[26] P.-H. Huang, Y.-H. Wang, J.-C. Ke, and C.-J. Huang, Energies **10**, 599 (2017).

[27] L. Xie, H. Hwang, M. Kim, and K. Kim, Phys. Chem. Chem. Phys. **19**, 1143 (2017).

[28] C. Ma, C. Leng, Y. Ji, X. Wei, K. Sun, L. Tang, J. Yang, W. Luo, C. Li, Y. Deng, S. Feng, J. Shen, S. Lu, C. Du, and H. Shi, Nanoscale **8**, 18309 (2016).

[29] S.M. Jain, B. Philippe, E.M.J. Johansson, B. Park, H. Rensmo, T. Edvinsson, and G. Boschloo, J. Mater. Chem. A **4**, 2630 (2016).

[30] T. Supasai, N. Rujisamphan, K. Ullrich, A. Chemseddine, and T. Dittrich, Appl. Phys. Lett. **103**, (2013).

[31] A.O. Juma, A. Azarpira, A. Steigert, M. Pomaska, C.-H. Fischer, I. Lauermann, and T. Dittrich, J. Appl. Phys. Addit. Inf. J. Appl. Phys. J. Homepage **114**, 2 (2013).

[32] P. Prajongtat and T. Dittrich, J. Phys. Chem. C **119**, 9926 (2015).

[33] A.K. Jena, Y. Numata, M. Ikegami, and T. Miyasaka, J. Mater. Chem. A **6**. 2219 (2018).

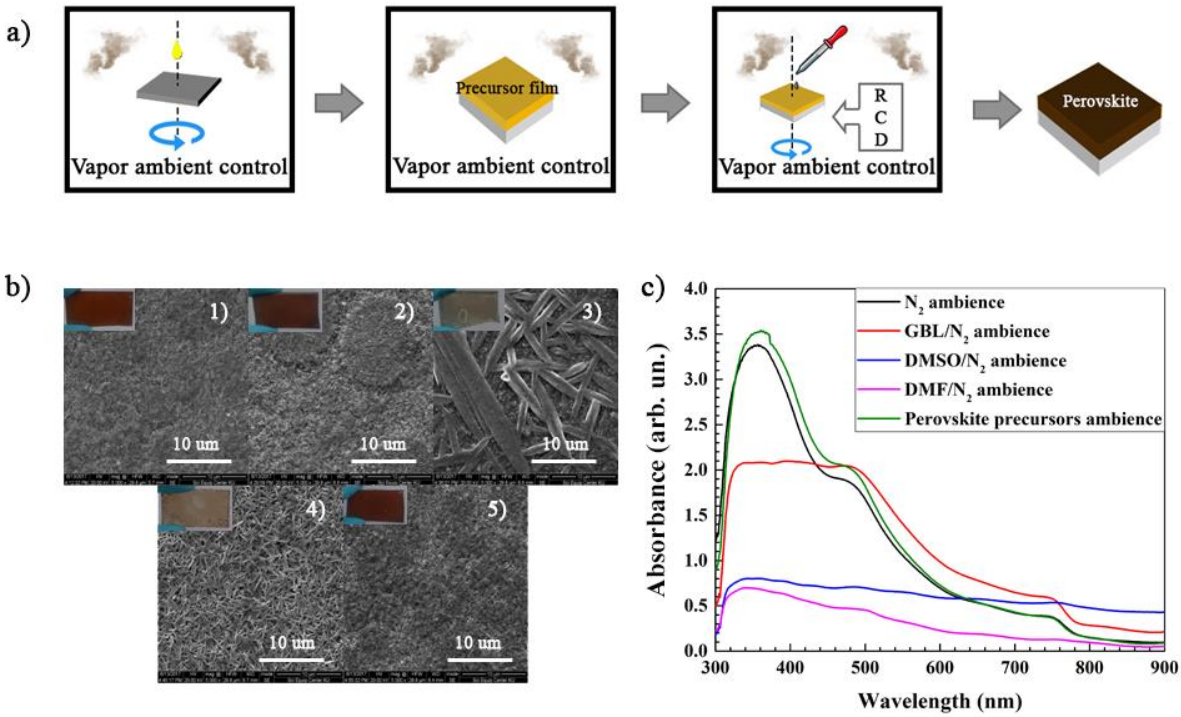

Figure 1: (a) Diagram of repeated cation doping (RCD) method. (b) SEM images of perovskite films formed under N_2, GBL/N_2, DMSO/N_2, DMF/N_2, and perovskite precursors/N_2 ambiences respectively with optical images as insets. (c) Absorption spectra of perovskite films.

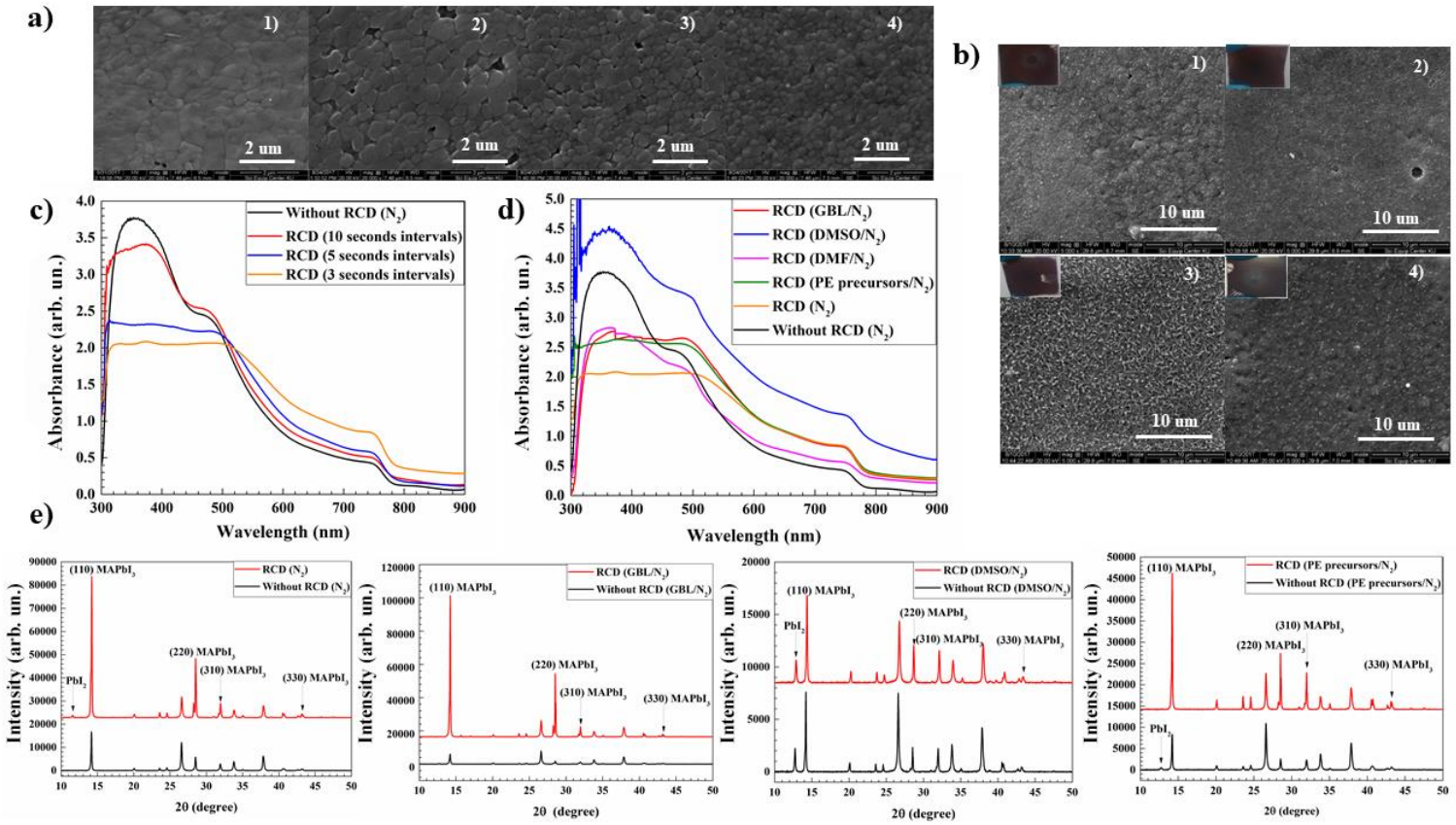

Figure 2: (a) SEM images of perovskite film in N_2 ambience without RCD and with RCD using 10 second, 5 second, and 3 second intervals, respectively. (b) SEM images of perovskite films with RCD using 3 second interval in GBL/N_2, DMSO/N_2, DMF/N_2, and PE precursors/N_2 ambiences. (c) Absorption spectra of perovskite films with RCD using 10 s, 5 s, and 3 s intervals. (d) Absorption spectra of perovskite films with RCD using 3 seconds interval in N_2, GBL/N_2, DMSO/N_2, DMF/N_2, and Perovskite precursors/N_2 ambiences. (e) XRD of perovskite film with and without RCD on TiO_2/FTO.

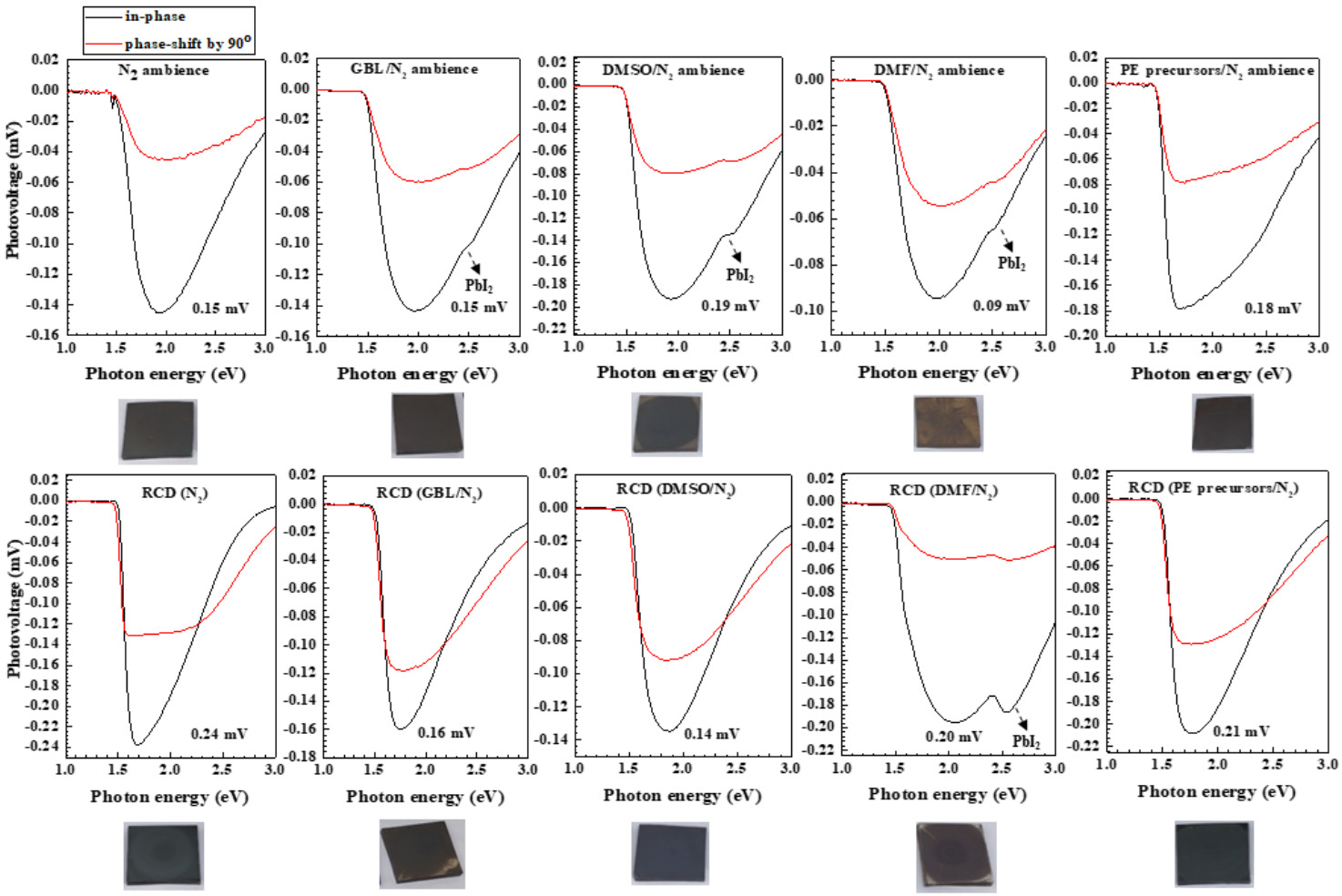

Figure 3: SPV spectra of perovskite films in ambiences from left to right; N_2, GBL/N_2, DMSO/N_2, DMF/N_2, and Perovskite precursors/N_2. Upper row: without RCD; lower row: with RCD.

AMBIENCE	W-W/O RCD	E_t (meV)
N_2	W/O RCD	23
	RCD – 10 sec intervals	21
	RCD – 5 sec intervals	22
	RCD – 3 sec intervals	17
GBL/N_2	W/O RCD	27
	RCD – 3 sec intervals	23
DMSO/N_2	W/O RCD	21
	RCD – 3 sec intervals	22
DMF/N_2	W/O RCD	24
	RCD – 3 sec intervals	25
PE PRECURSORS/N_2	W/O RCD	21
	RCD – 3 sec intervals	21

Table 1: The characteristic energies of tail defect state (E_t) measurements for perovskite films in ambiences without RCD and with RCD. The fitting and calculation were shown in the supplementary information.

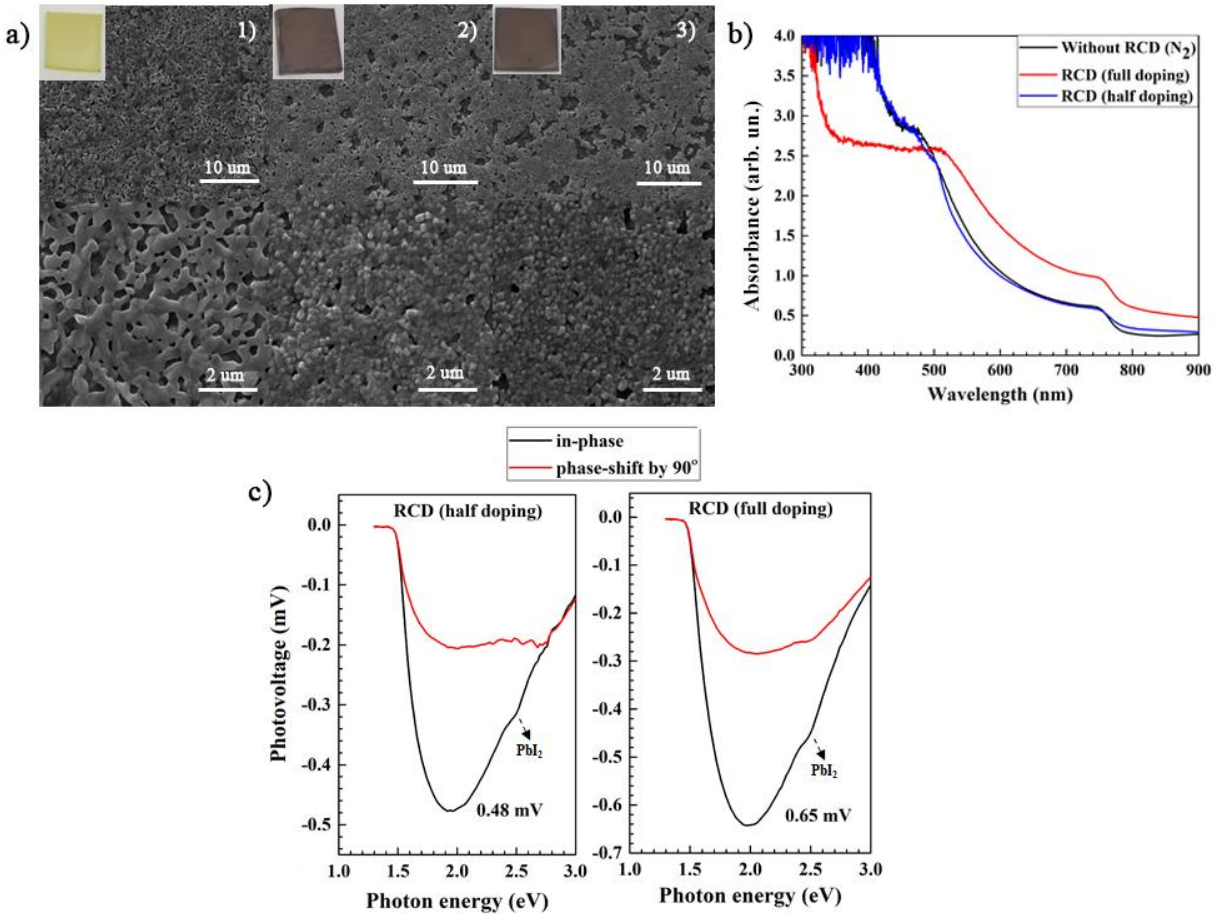

Figure 4: (a) SEM of wasted perovskite films (left) and recycled perovskite films with RCD using half doping (middle) and full doping (right) (b) Absorption spectra of recycled perovskite films. The black line is a regular perovskite control sample for comparison. (c) SPV spectra of recycled perovskite films.

Supporting information

The linear-scale data plots (left) showed spectra of the normalized squared SPV amplitudes of the samples fabricated without/with RCD in different ambiences. All samples indicated onset energies (E_{on}) in the range close to the reported perovskite band gap (E_g) (～1.5 eV)[1] , except the perovskite film that was fabricated in DMF/N_2 vapor ambience without RCD technique had its band gap shifted to ～1.6 eV.

The exponential tails of the SPV data below the band gap contain information about charge separation from defect states near the valence band. The logarithmic-scale data plots (right) of the perovskite films fabricated without/with RCD in different ambiences could be fitted to determine the characteristic energies of tail defect states (E_t). The characteristic energy, also called energy of the exponential tails indicates the disorder caused by electronic state. The technique is expansively explained in previous work [2, 3]. We briefly summarized the method below.

The amplitude of the SPV signal is calculated as the square root of the sum of the squares of the X signal (in – phase) and the Y signal (phase – shifted by 90 degrees). The square root is then divided by photon flux (ϕ). E_t was then obtained by fitting the following equation[2] :

$$\frac{\text{SPV amplitude}}{\text{flux}} = A \exp\left(\frac{h\nu}{E_t}\right),$$

where A is a proportionality constant.

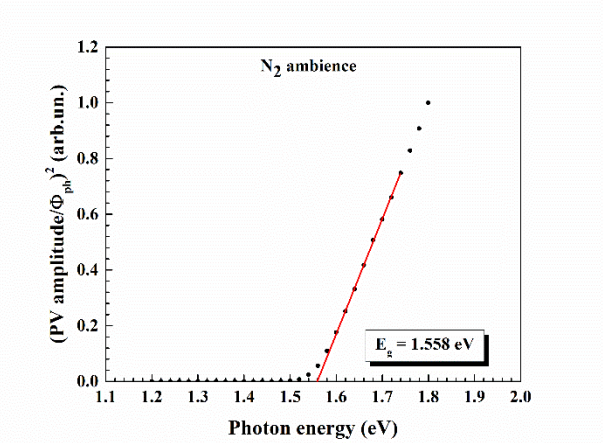
N2 ambience
(PV amplitude/Φph)2 (arb.un.)
Eg = 1.558 eV
Photon energy (eV)

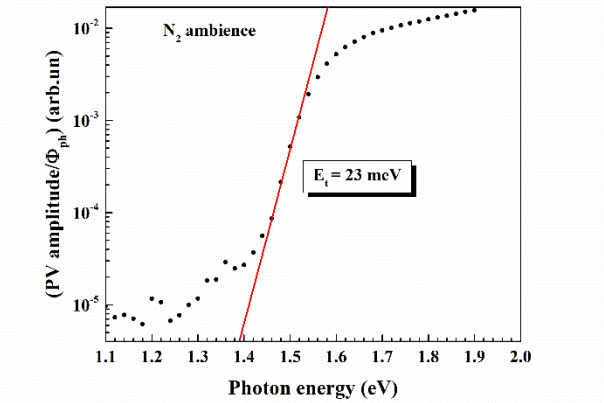
N2 ambience
(PV amplitude/Φph) (arb.un)
Et = 23 mcV
Photon energy (eV)

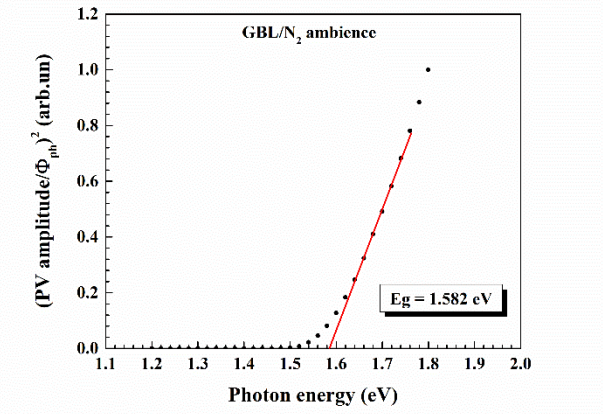
GBL/N2 ambience
(PV amplitude/Φph)2 (arb.un)
Eg = 1.582 eV
Photon energy (eV)

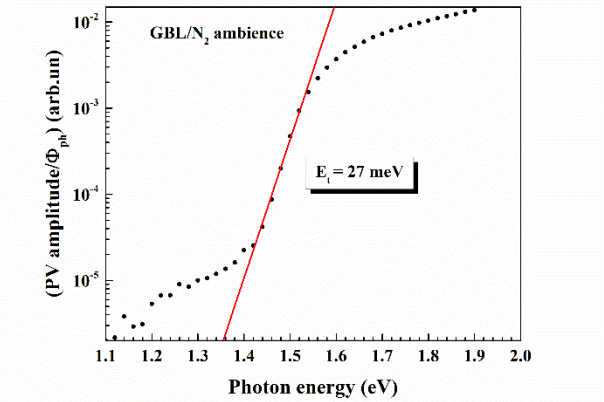
GBL/N2 ambience
(PV amplitude/Φph) (arb.un)
Et = 27 meV
Photon energy (eV)

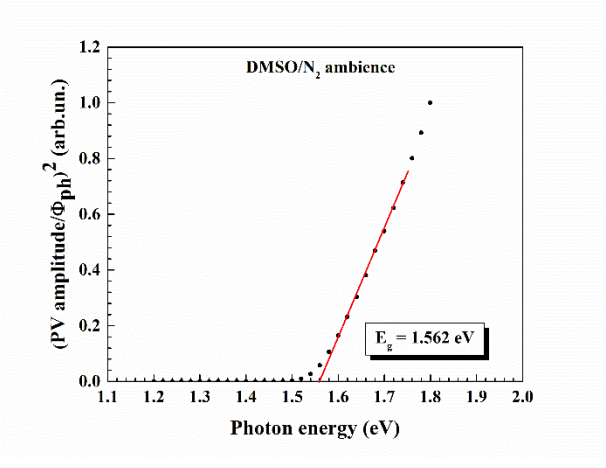
DMSO/N2 ambience
(PV amplitude/Φph)2 (arb.un.)
Eg = 1.562 eV
Photon energy (eV)

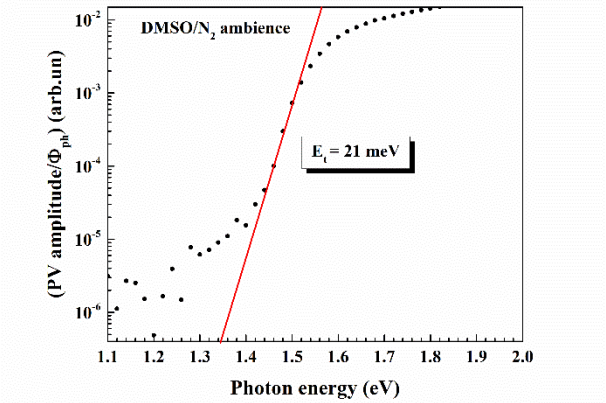
DMSO/N2 ambience
(PV amplitude/Φph) (arb.un)
Et = 21 meV
Photon energy (eV)

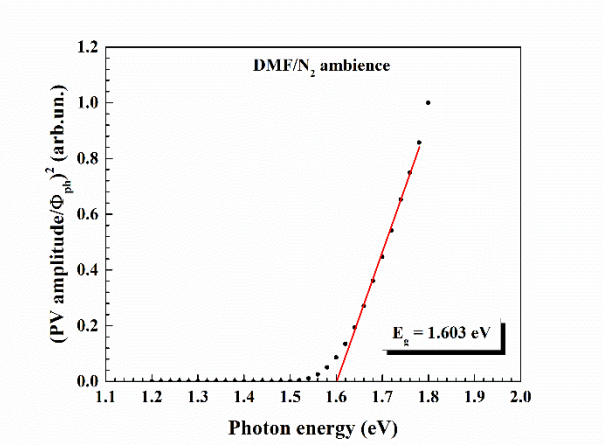
DMF/N2 ambience
(PV amplitude/Φph)2 (arb.un.)
Eg = 1.603 eV
Photon energy (eV)

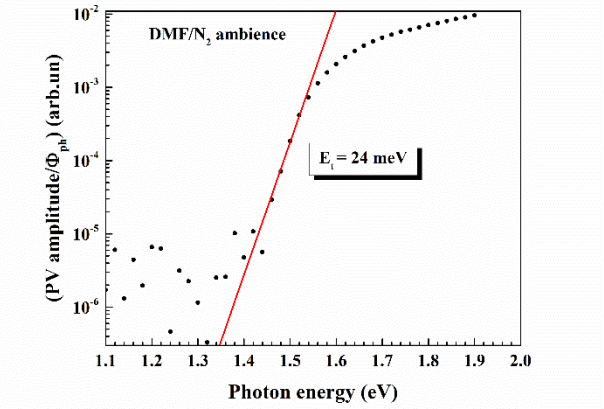
DMF/N2 ambience
(PV amplitude/Φph) (arb.un)
Et = 24 meV
Photon energy (eV)

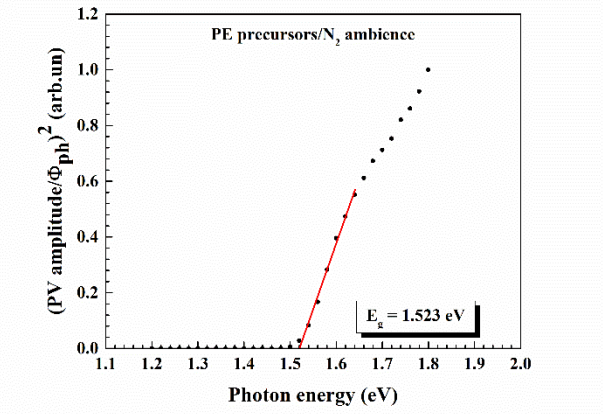
PE precursors/N2 ambience
(PV amplitude/Φph)2 (arb.un)
Eg = 1.523 eV
Photon energy (eV)

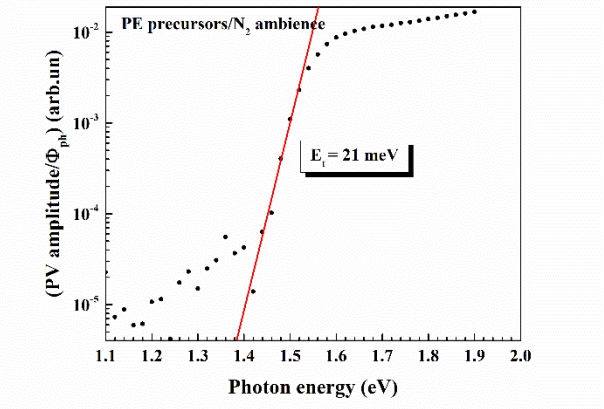
PE precursors/N2 ambience
(PV amplitude/Φph) (arb.un)
Et = 21 meV
Photon energy (eV)

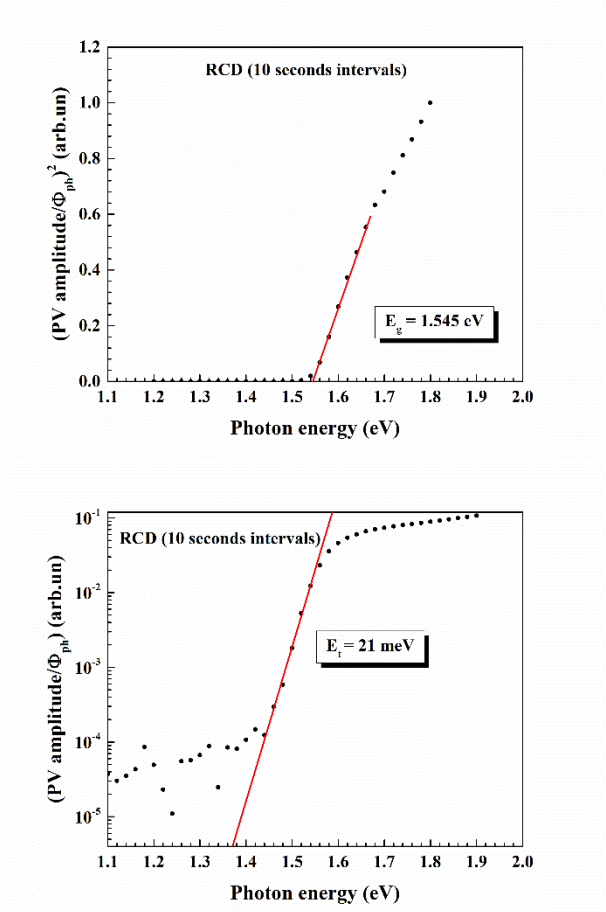
RCD (10 seconds intervals)
E_g = 1.545 eV
$(PV\ amplitude/\Phi_{ph})^2$ (arb.un)
Photon energy (eV)

RCD (10 seconds intervals)
E_τ = 21 meV
$(PV\ amplitude/\Phi_{ph})$ (arb.un)
Photon energy (eV)

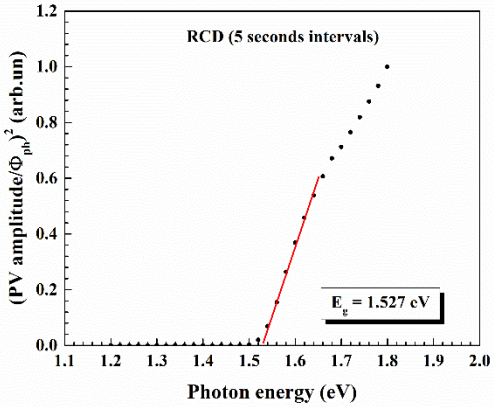
RCD (5 seconds intervals)
E_g = 1.527 eV
(PV amplitude/Φ_{ph})^2 (arb.un)
Photon energy (eV)

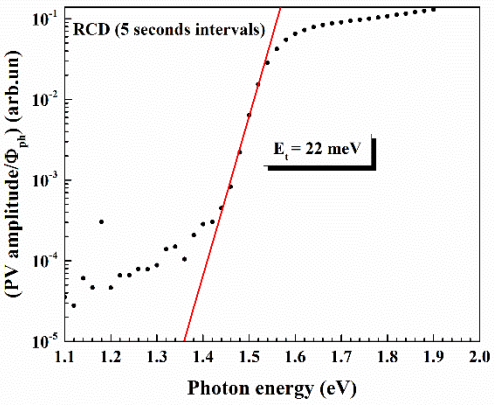
RCD (5 seconds intervals)
E_t = 22 meV
(PV amplitude/Φ_{ph}) (arb.un)
Photon energy (eV)

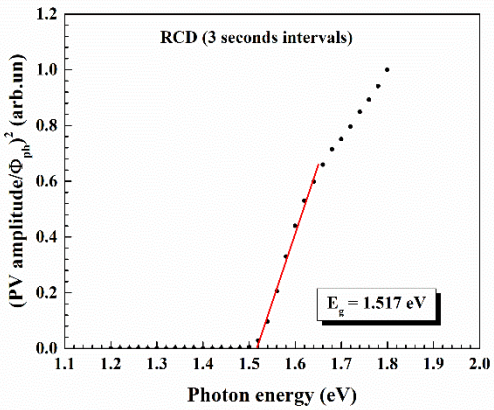
RCD (3 seconds intervals)
E_g = 1.517 eV
(PV amplitude/Φ_{ph})^2 (arb.un)
Photon energy (eV)

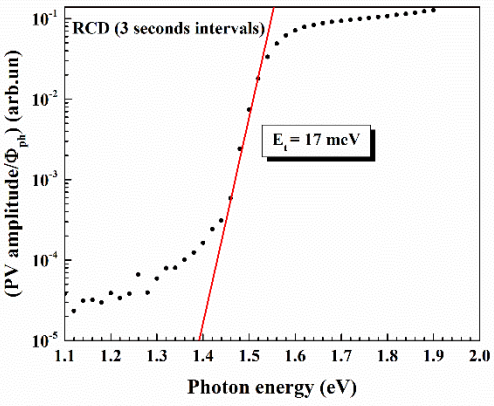
RCD (3 seconds intervals)
E_t = 17 mcV
(PV amplitude/Φ_{ph}) (arb.un)
Photon energy (eV)

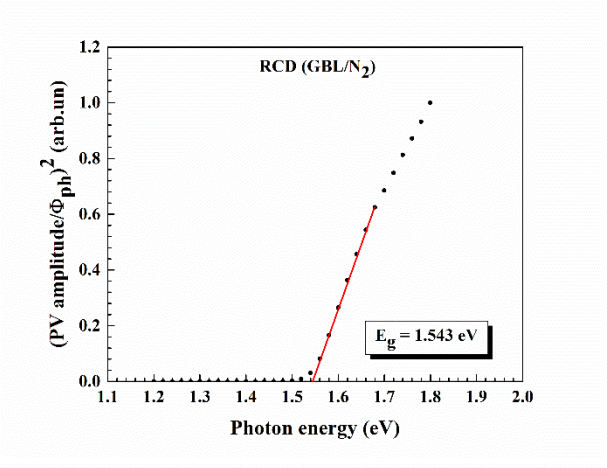
RCD (GBL/N2)
(PV amplitude/Φph)2 (arb.un)
Eg = 1.543 eV
Photon energy (eV)

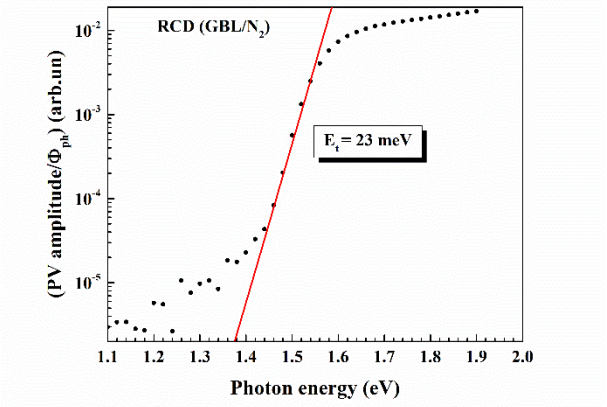
RCD (GBL/N2)
(PV amplitude/Φph) (arb.un)
Et = 23 meV
Photon energy (eV)

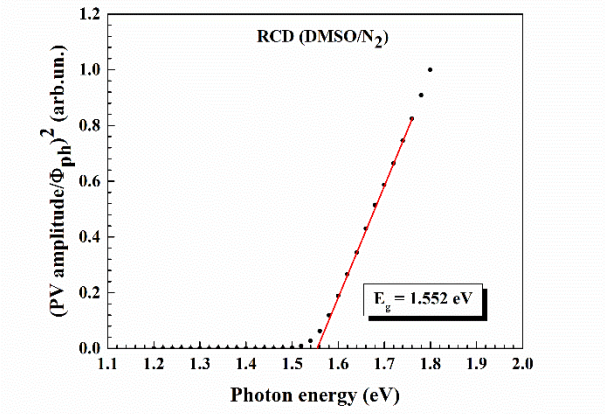
RCD (DMSO/N2)
(PV amplitude/Φph)2 (arb.un.)
Eg = 1.552 eV
Photon energy (eV)

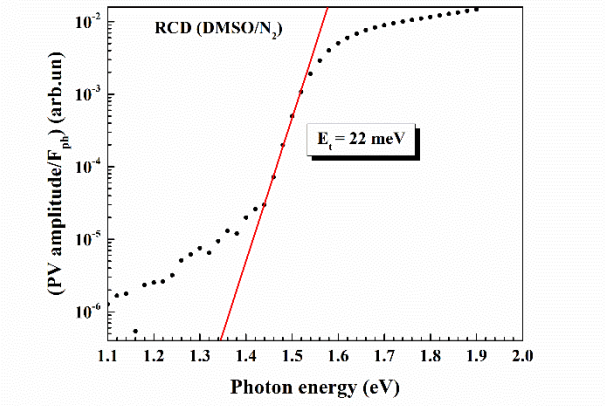
RCD (DMSO/N2)
(PV amplitude/Fph) (arb.un)
Et = 22 meV
Photon energy (eV)

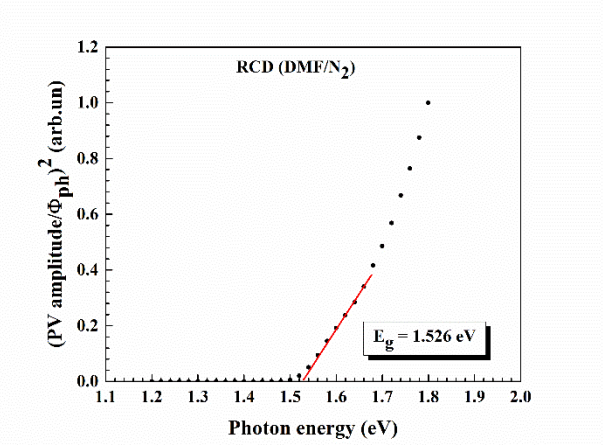
RCD (DMF/N2)
(PV amplitude/Φph)2 (arb.un)
Eg = 1.526 eV
Photon energy (eV)

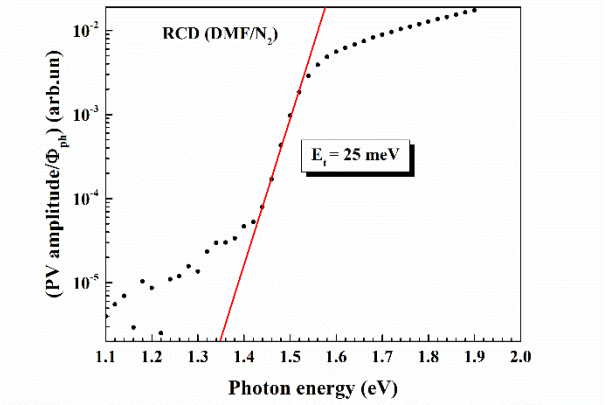
RCD (DMF/N2)
(PV amplitude/Φph) (arb.un)
Et = 25 meV
Photon energy (eV)

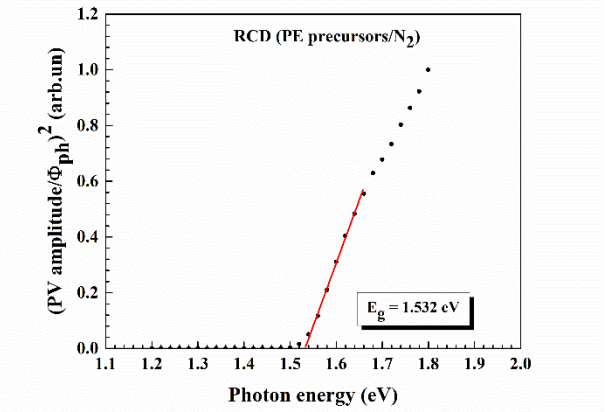
RCD (PE precursors/N2)
(PV amplitude/Φph)2 (arb.un)
Eg = 1.532 eV
Photon energy (eV)

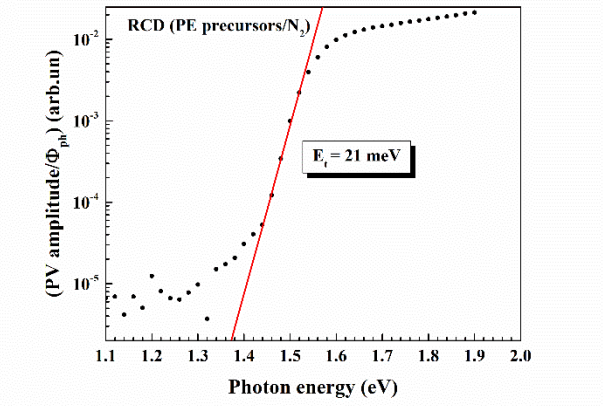
RCD (PE precursors/N2)
(PV amplitude/Φph) (arb.un)
Et = 21 meV
Photon energy (eV)

References

1. Supasai T, Rujisamphan N, Ullrich K, et al (2013) Formation of a passivating CH3NH3PbI 3/PbI2 interface during moderate heating of CH 3NH3PbI3 layers. Appl Phys Lett 103: . doi: 10.1063/1.4826116

2. Juma AO, Azarpira A, Steigert A, et al (2013) Role of chlorine in In2S3 for band alignment at nanoporous-TiO2/In2S3 interfaces Role of chlorine in In 2 S 3 for band alignment at nanoporous-TiO 2 /In 2 S 3 interfaces. J Appl Phys Addit Inf J Appl Phys J Homepage 114:2–7 . doi: 10.1063/1.4817766doi.org/10.1063/1.4817766

3. Prajongtat P, Dittrich T (2015) Precipitation of $CH_3NH_3PbCl_3$ in $CH_3NH_3PbI_3$ and Its Impact on Modulated Charge Separation. J Phys Chem C 119:9926–9933 . doi: 10.1021/acs.jpcc.5b01667

6. Output (Acknowledge the Thailand Research Fund)

6.1 International Journal Publication

4 international publications acknowledging the Thailand Research Fund.

1 paper as the corresponding author.

1) Boonthum, C., Pinsuwan, K., Ponchai, J., Srikhirin, T., & **Kanjanaboos, P. *** *Reconditioning Perovskite films under Vapor Environments through Repeated Cation Doping* **Applied Physics Express** 2018 ASAP (Impact factor **2.67**)

3 papers as the co-author

1) Griesemer, S., You, S., **Kanjanaboos, P.,** Calabro, M., Jaeger, H. M., Rice, S. A., & Lin B.***** *The role of ligands in the mechanical properties of Langmuir nanoparticle films* **Soft Matter** 2017, **13**, 3125-3133 (Impact factor **3.89**)
2) Wang, R., Shang, Y., **Kanjanaboos P.**, Wenjia Z., Ning Z., Sargent, E.H.***** *Colloidal Quantum Dot Ligand Engineering for High Performance Solar Cells* **Energy & Environmental Science** 2016, **9**, 1130-1143 (Impact factor **29.52**)
3) Shaikh, J. S., Shaikh, N. S., Sheikh, A.D., Mali, S. S., Kale, A. J., **Kanjanaboos P.,** Hong, C. K., Kim. J. H. & Patil, P. S.***** *Perovskite solar cells: In pursuit of efficiency and stability* **Materials & Design** 2017, **136**, 54-80 (Impact factor **3.5**)

6.2 Research Utilization and Application

Commercial impact

The work developed new technology to help actual future production by improving the quality of perovskites for optoelectronic applications through the RCD process.

Academic impact

This work also created a new researcher (a master student who is the first author for the work published in APEX). Publications from this grant are useful for researchers in the field around the world and our own academic work regarding perovskite solar cells. The experimental methods optimized in the work were also adapt for laboratory coursework (SCME382) for undergraduate students in materials science.

Public impact and policy impact

N/A